University of Glasgow | School of Life Sciences

Quantification of the Variable Radiocarpal Ligaments Pattern

Radi Ali Al Saffar
Matriculation No. 1004752

Supervised by: Dr Quentin Fogg

University of Glasgow

Declaration of Originality Form

Name: RADI ALI AL SAFFAR.
Student Number: 1004752.
Course Name: MSc ORTHOPAEDIC ANATOMY.
Assignment Number/Name: QUANTIFICATION OF THE VARIABLE RADIOCARPAL LIGAMENTS PATTERN.

I confirm that this assignment is my own work and that I have:

- Read and understood the guidance on plagiarism in the Undergraduate Handbook, including the University of Glasgow Statement on Plagiarism ☐
- Clearly referenced, in both the text and the bibliography or references, **all sources** used in the work ☐
- Fully referenced (including page numbers) and used inverted commas for **all text quoted** from books, journals, web etc. (Please check the section on referencing in the 'Guide to Writing Essays & Reports' appendix of the Graduate School Research Training Programme handbook.) ☐
- Provided the sources for all tables, figures, data etc. that are not my own work ☐
- Not made use of the work of any other student(s) past or present without acknowledgement. This includes any of my own work, that has been previously, or concurrently, submitted for assessment, either at this or any other educational institution, including school (see overleaf at 31.2) ☐
- Not sought or used the services of any professional agencies to produce this work ☐

In addition, I understand that any false claim in respect of this work will result in disciplinary action in accordance with University regulations ☐

DECLARATION:
I am aware of and understand the University's policy on plagiarism and I certify that this assignment is my own work**,** except where indicated by referencing, and that I have followed the good academic practices noted above

Signed...

Acknowledgments

As always, my eternal gratitude goes to the Almighty God, the fountain of all wisdom and understanding, for shining His glorious light in my path throughout the duration of the research and especially while I pursued this dissertation.

My deep gratitude must go to ***Dr Quentin Fogg****, supervisor of this project, for all his help and support.*

Many thanks also to ***Prof. Mohammed Almutabagani****, for his help, thoughts and enthusiasm throughout the year.*

Indefinite thanks to my princess, ***Layla****, and my little son,* ***Basim****, for their love and support throughout my study.*

Special thanks to all of my family members and friends (in UK and Saudi Arabia) for their support and motivation.

Mr. Andy Lockhart *and* ***Mr.David Russell*** *for their help during specimen preparation.*

All cheerful staff at the department of Anatomy, for their unlimited help and co-operation.

All the donors and their families from the West of Scotland Body Donation Programme.

Radi AL Saffar

Contents

Abbreviations

2D Two-dimensional.
3D Three-dimensional.

A
A Area.
A/L Index area.

C
C Capitate.
CIC Carpal instability complex.
CID Carpal instability dissociative.
CIND Carpal instability non-dissociative.

D
DDRU Doral distal radioulnar ligament.
DISI Dorsal intercalated segment instability.
DPX Di-N-Butyle Phthalate in Xylene.
DRC Dorsal radiocarpal ligament.

E
EDTA Ethylenediaminetetraacetic acid.

F
TFCC Triangular fibrocartilage complex.

H
H Hamate.

K
K-wire Kirschner wire.

L
L Length.
L Lunate.
Ld Distal lunate attachment.
Lm Middle length.
Lp Proximal lunate attachment.
Lr Radial length.
LRL Long radiolunate ligament.
LT Lunotriquetral ligament.
LTiO Lunotriquetral interosseous ligament.
Lu Ulnar length.

P
P Perimeter.
P Pisiform.
P/L Index perimeter.
PDRU Palmar distal radioulnal ligament.
PISI Palmar intercalated segment instability.

R
R Radius.
R.A. Radi Al Saffar.
RC Radiocapitate ligament.
RC-H Radiocapitohamate ligament.
RCL Radial collateral ligament.
RL Radiolunate ligament.
RLT Radiolunotriquetral ligament/band.
RR Radioradial ligament.
RS Radioscaphoid ligament.
RSC Radioscaphocapitate ligament.
RSC-T Radioscaphocapitate ligament with a triquetral band.
RSC-TH Radioscaphocapitate ligament with triquetrum and hamate attachments.
RSL Radioscapholunate ligament.
RS-Tm Radioscaphotrapezial ligament.
RT Radiotriquetral ligament/band.
R-TFCC Radio-triangular fibrocartilage complex ligament.

S
S Scaphoid.
Sd Distal scaphoid attachment.
SLiO Scapholunate inetrosseous ligament.
Sp Proximal scaphoid attachment.
SRL Short radiolunate ligament.
ST Scapho-trapezial ligament.

T
T Triquetrum.
TFCC Triangular fibrocartilage complex.
Tm Trapezium.

U
U Ulna.

W
Wd Distal width.
Wm Middle width.
Wp Proximal width.

Log of Investigation

The idea:

I have a strong interest in the small joints of the hand as they are of high clinical importance. I chose orthopaedic anatomy because of the relative link between the Anatomy as a basic subject and the clinical aspect of Orthopaedics, which expand the horizon for further specialisation.

Final topic:

I was looking for a challenging topic to pursue my MSc and proceed towards PhD in a similar field. After a personal communication with Dr Quentin Fogg, radiocarpal ligaments were chosen as the broad topic of the research. It is a competitive project as the literature is relatively poor whenever considering related topics to wrist instability and radiocarpal ligaments.

Literature research strategies:

Two main databases: “Pubmed” and ‘’Web of Knowledge ‘’ were used. The initial search term was “radiocarpal ligaments” which returned 199 and 290 articles in Pubmed and Web of Knowledge respectively. The initial research focused on recent articles reviewing the core interest of this work to come to a broad understanding of the topic. Various general articles were selected from respected journals as an initial step, followed by selecting relevant papers from the reference list. Subsequently, the search was modified according to the focus of the research.

Additional strategies:

The early results of this project were presented and discussed at the 11th Congress of European Association of Clinical Anatomy (EACA) held jointly with Summer Meeting of British Association of Clinical Anatomists (BACA) Padua, June 29 - July 1, 2011. The Final results were presented and discussed in the second Glasgow Orthopaedic Research Initiative meeting, October 6, 2011.

Uniqueness of the topic:

The originality of this dissertation is attributed to its aim to identify ligamentous structures following strict criteria using various modes of research that were poorly represented in the literature. Obviously, a huge amount of interest and work has been already dedicated in dissecting the carpal ligaments and identifying their actual attachments. However, this dissertation uniquely focused on the radiocarpal ligaments, looking at the variability in their attachment with a quantitative analysis, and in assessing whether previous works were credible.

Publications Related to This Research

<u>1. Poster presentation</u>:

Quantitative 3D Investigation of ligamentous attachments to the distal radius;

11th Congress of European Association of Clinical Anatomy (EACA) held jointly with Summer Meeting of British Association of Clinical Anatomists (BACA); Padua, June 29 - July 1, 2011.

<u>2. Platform presentation:</u>

Radiocarpal Interactions Demonstrated Quantitatively with 3D Microscribe Reconstruction;

Second Glasgow Orthopaedic Research Initiative (GLORI) meeting; University of Strathclyde, October 6, 2011.

Abstract

Background: The connections between the radius and the forearm, supporting the radiocarpal joint are poorly understood. They are also of high clinical importance as they are easily damaged through trauma and involved in the mechanical/functional decline of wrists with various degenerative joint diseases. This area has been a source of debate and inconsistency for decades due to the lack of reproducible, quantitative studies, and the recurrent use of different descriptions and terminology. The current study aims to accurately define the key ligaments supporting the radiocarpal joint by quantifying the size, shape and attachment area of the ligamentous structures around the distal radius.

Materials and Methods: The various attachments of each radiocarpal ligament were analysed in 10 anatomic preparations using gross, histological and 3D morphometric approaches. Each ligament fascicular pattern was traced from one attachment to another; diversions into non-fascicular (disorganised) tissue were excised. The dimensions of each ligament were measured three different ways: manual with callipers, from a digital photograph using ImageJ and with a 3D digitizer to create and measure a virtual 3D model of each structure. Two parameters were analysed in three different levels: the radial, middle and ulnar length as well as the proximal, middle and distal width. The area of ligamentous attachment (enthesis) of each radiocarpal ligament was measured with the microscribe digitiser and confirmed histologically.

Results: The ligamentous attachments of the distal radius are highly variable. Unlike the manual and digital measurements, microscribe measurements provide more reproducible data as there was no significant difference between the rounds of measurement for all structures ($p>0.05$). Histological analysis confirmed the gross findings with more quantitative details about each attachment.

Conclusions: These results provide an important insight towards a better understanding of the complex radiocarpal ligament anatomy with a morphometric description. The microscribe method gave more consistent results than the manual and digital methods and it is probably more accurate. The current study may suggest a special consideration in relation to the carpal instability aetiology and management. Further studies are required to determine the causative factors of these variations besides the study approaches and individual variability.

Introduction

The variability of the anatomy of the ligaments of the wrist has been investigated in the literature (Mayfield *et al.*, 1976; Berger and Landsmeer, 1990; Theumann *et al.*, 2003; Nagao *et al.*, 2005; Kijima and Viegas, 2009; Nanno and Viegas, 2009). However, a lack of consensus on the classification, terminology and investigative techniques has hindered the reproducibility of these studies (Feipel and Rooze, 1999; Theumann *et al.*, 2003; Kijima and Viegas, 2009). The result is a complicated, unclear and inconsistent collection of studies on wrist ligaments (Berger, 1997). Among these ligaments are the radiocarpal ligaments, which were particularly poorly defined in the literature. Variable patterns of ligamentous connections may influence the biomechanical properties as well as the stability of a joint (Shin *et al.*, 2000; Tang, 2008; McLean *et al.*, 2009). As such, a comprehensive knowledge of the osseous and ligamentous anatomy of the radiocarpal ligaments is essential for improved understanding of carpal instability and pathomechanics (Dobyns and Gabel, 1990; Trail *et al.*, 2007; Carlsen and Shin, 2008).

Enthesial Anatomy

Better understanding of ligament patterns alone is insufficient to fully understand the wrist. It is also important to understand where and how individual ligaments are attached to bone. The bony attachments of ligaments are called "entheses" or "osteoligamentous junctions". It is worth knowing that the entheses are common targets for overuse injuries as well as a collection of rheumatic diseases called seronegative spondyloarthropathies (Benjamin and Ralphs, 1998; Benjamin and McGonagle, 2001; Benjamin *et al.*, 2004). Moreover, they are of high clinical importance whenever surgeons need to reattach a torn ligament to a bone (Benjamin *et al.*, 2006; Benjamin and McGonagle, 2009). Studying the morphology of the entheses provides a critical insight into the pathomechanics of joint diseases (Benjamin *et al.*, 1986; Camus *et al.*, 2004; Majima *et al.*, 2008). Accordingly, it may enhance not only the assessment and diagnosis of ligamentous disruption, but also understanding and treating carpal instability (Palmer *et al.*, 1978; Camus *et al.*, 2004; Galtes *et al.*, 2006; Kawamura and Chung, 2007).

Ligamentous Anatomy

The wrist has a complex anatomy. This complexity is exaggerated due to the number of the structures that have been reported using variable terminology (Mayfield *et al.*, 1976; Berger and Landsmeer, 1990; Theumann *et al.*, 2003; Nagao *et al.*, 2005; Kijima and Viegas, 2009; Nanno and Viegas, 2009). This is undoubtedly true in case of the carpal ligaments (Berger, 1997). The carpal ligaments can be classified according to their fundamental histological features. As a result, two distinct groups of carpal ligaments have been identified: the capsular (extrinsic) and intra-articular (intrinsic) ligaments. Further subdivision of these types can be obtained when considering the tissue composition (Berger, 1997). The current study will focus upon extrinsic ligaments; specifically, the radiocarpal ligaments. The lack of consensus on their arrangement is indicative of how difficult it is to separate them from non-ligamentous capsular tissue (Berger and Blair, 1984; Berger et al., 1984; Carlsen and Shin, 2008).

Inconsistencies are found between several authors’ descriptions of extrinsic wrist ligaments (Mayfield *et al.*, 1976; Berger and Landsmeer, 1990; Theumann *et al.*, 2003; Nagao *et al.*, 2005; Kijima and Viegas, 2009; Nanno and Viegas, 2009). This makes comparisons between studies difficult. Microscopically, both capsular and intra-articular ligaments have the same basic configuration. A ligament can be defined as longitudinally arranged groups of fascicles connecting two or more structures along a (force-) specific path, with each fascicle composed of dense and finely organised collagen fibres (Berger and Blair, 1984). Failure to consistently apply such a definition to ligamentous studies may be one source of observer variation. For the current study, this definition will be applied to the radiocarpal ligaments.

Anatomy of Radiocarpal Ligaments:

The distal radius has a series of fibrous tissue connections to the ulna, triangular fibrocartilage complex (TFCC), tendon sheaths and a number of carpal bones (Feipel and Rooze, 1999; Theumann *et al.*, 2003; Nanno *et al.*, 2006; Kijima and Viegas, 2009; Nanno and Viegas, 2009). These connections are likely to vary with different modes of carpal, TFCC and distal radioulnar joint type and/or function (Feipel and Rooze, 1999; Theumann *et al.*, 2003; Kijima and Viegas, 2009). The anatomy of various radiocarpal ligament patterns has been described in the literature (Mayfield *et al.*, 1976; Berger and Landsmeer, 1990; Theumann *et al.*, 2003; Nagao *et al.*, 2005; Kijima and Viegas, 2009; Nanno and Viegas, 2009). The radiocarpal ligaments fall into two distinct categories according to their anatomical location, the palmar and dorsal radiocarpal ligaments. In addition, the radial collateral ligament (RCL) is included in some discussions.

1. Palmar Radiocarpal Ligaments:

Variable descriptions of the palmar radiocarpal ligaments were reported using different modalities (Figure 1) (Mayfield *et al.*, 1976; Berger and Landsmeer, 1990; Theumann *et al.*, 2003; Nagao *et al.*, 2005; Kijima and Viegas, 2009; Nanno and Viegas, 2009). Three major radial connections to the capitate, scaphoid and lunate were identified. These connections are highly variable and suggest different patterns of ligamentous attachments, not only between the distal radius and the carpal bones, but also to the TFCC and the adjacent sheaths (Mayfield *et al.*, 1976; Berger and Landsmeer, 1990; Theumann *et al.*, 2003; Nagao *et al.*, 2005; Kijima and Viegas, 2009; Nanno and Viegas, 2009).

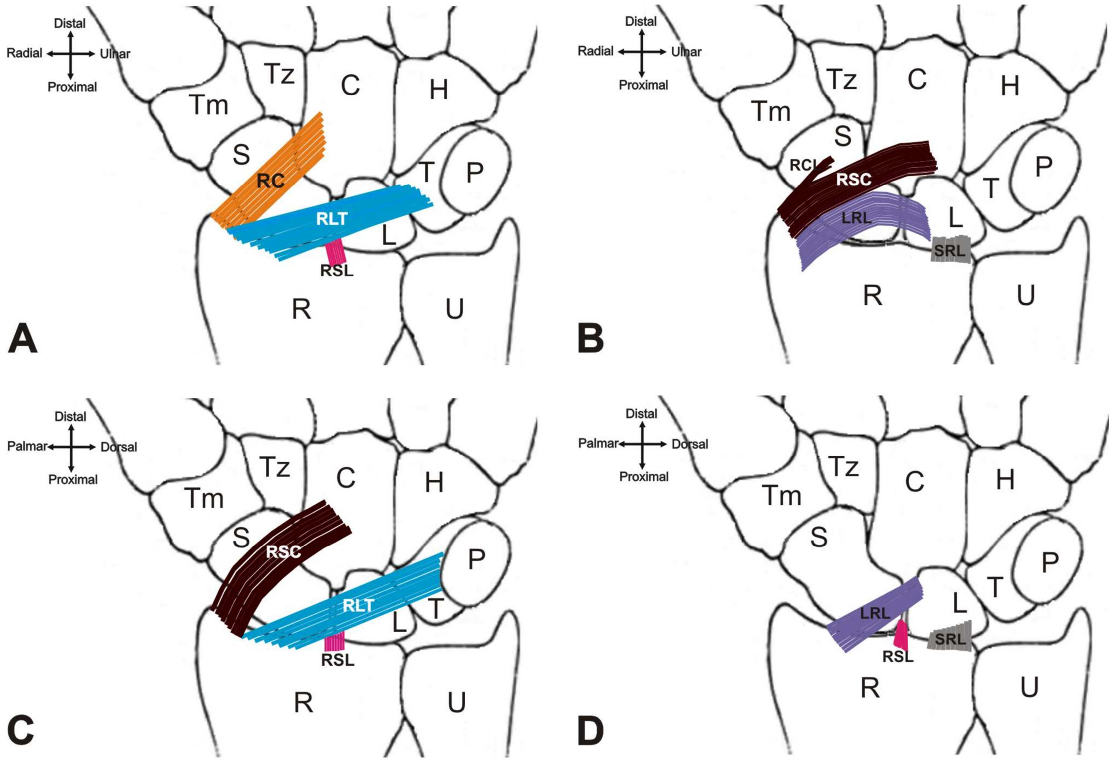

Figure 1. Variable palmar radiocarpal ligaments pattern reported in the literature. **A.** Reported by Mayfield *et al.* (1976). **B**. Reported by Berger and Landsmeer (1990), note the radial collateral ligament (RCL) branching from the most radial fibres of the radioscaphocapitate ligament (RSC). **C.** Reported by Theumann *et al.* (2003). **D.** Radiocarpal ligaments around the lunate reported by Nagao *et al.* (2005). RC= radiocapitate ligament, RSC= radioscaphocapitate ligament, RSL= radioscapholunate ligament, RCL= radial collateral ligament, LRL= long radiolunate ligaments, SRL= short radiolunate ligament, RLT=radiolunotriquetral ligament, R= radius, U= ulna, S= scaphoid, L= lunate, T= triquetrum, P= pisiform, Tm= trapezium, Tz= trapezoid, C= Capitate and H=hamate.

1.1 Radiocapitate connections:

Two distinct radiocapitate ligaments have been described in the literature (Figure 1); the radiocapitate ligament (RC) (Mayfield *et al.*, 1976; Berger and Blair, 1984; Berger *et al.*, 1984; Feipel and Rooze, 1999) and the radioscaphocapitate ligament (RSC) (Mizuseki and Ikuta, 1989; Berger and Landsmeer, 1990; Theumann *et al.*, 2003; Kijima and Viegas, 2009). When one is reported, the other, if mentioned, is discredited, but no functional associations have been verified. Fogg (2004) proposed that these may be indicators of two functional subtypes.

1.2 Radioscaphoid connections:

The radioscaphoid ligament (RS) is also referred to in the literature as the radioscapholunate ligament (RSL) and ligament of Testut (Berger and Landsmeer, 1990). It is often argued whether it is a true ligament or just a neurovascular bundle devoid from any collagenous fibre. This debate still exists because of the paucity of reproducible descriptions as well as the inconsistent use of terminology. However, when identified, the RS was consistently described as a discrete vertically oriented band (Figure 1) (Mayfield *et al.*, 1976; Berger and Landsmeer, 1990; Theumann *et al.*, 2003; Nagao *et al.*, 2005). It was found to be thinner than the other ligaments so it was not considered as a major mechanical structure (Theumann *et al.*, 2003; Kijima and Viegas, 2009).

Other studies, however, failed to isolate the RSL as a discrete ligament as it was found to have no collagen fibres. It was described as the anterior interosseous nerve and artery intra-articular extension together with the radial artery combining to form this "ligament" (Berger and Landsmeer, 1990). It had a vertical orientation making the proximal (membranous) region of SLiO (Berger and Landsmeer, 1990).

1.3 Radiolunate connections:

The ligamentous structures connecting the distal radius to the lunate were a source of high variability in the literature. It was suggested that the radiolunate connection is represented by two ligaments; the LRL and the SRL (Figures 1B and D) (Berger and Landsmeer, 1990; Nagao *et al.*, 2005). While the RSC was found to partially overlapp the proximal LRL attachment, the LRL was identified overlapping the palmar region of the SLiO completely (Nagao *et al.*, 2005). Also, the SRL was found to be proximal to the ulnolunate and palmar and proximal parts of the lunotriquetral interosseous ligament (LTiO) (Kijima and Viegas, 2009).

One of the quantitative studies reported a variability of the radiolunate connection (Feipel and Rooze, 1999), describing a double radiolunate connection configuration; they were not named differently although they resembled the LRL and SRL configuration.

A single ligament that linked the radius to the lunate and the triquetrum, called the radiolunotriquetral ligament (RLT), was also identified and described as a synonym for the LRL (Figure 1C) (Theumann *et al.*, 2003) and radiotriquetral ligament (RT) (Figure 1A) (Mayfield *et al.*, 1976).

2. Dorsal Radiocarpal Ligaments

The dorsal radial connection to the carpal bones was reported to be represented by the dorsal radiocarpal ligament (DRC) (Mizuseki and Ikuta, 1989; Feipel and Rooze, 1999; Viegas *et al.*, 1999; Viegas, 2001). Variable patterns (Figure 2) (Mayfield *et al.*, 1976; Feipel and Rooze, 1999; Theumann *et al.*, 2003; Nagao *et al.*, 2005) and classification (Figure 3) (Mizuseki and Ikuta, 1989; Viegas *et al.*, 1999) of the DRC have been described but no consensus has been reached.

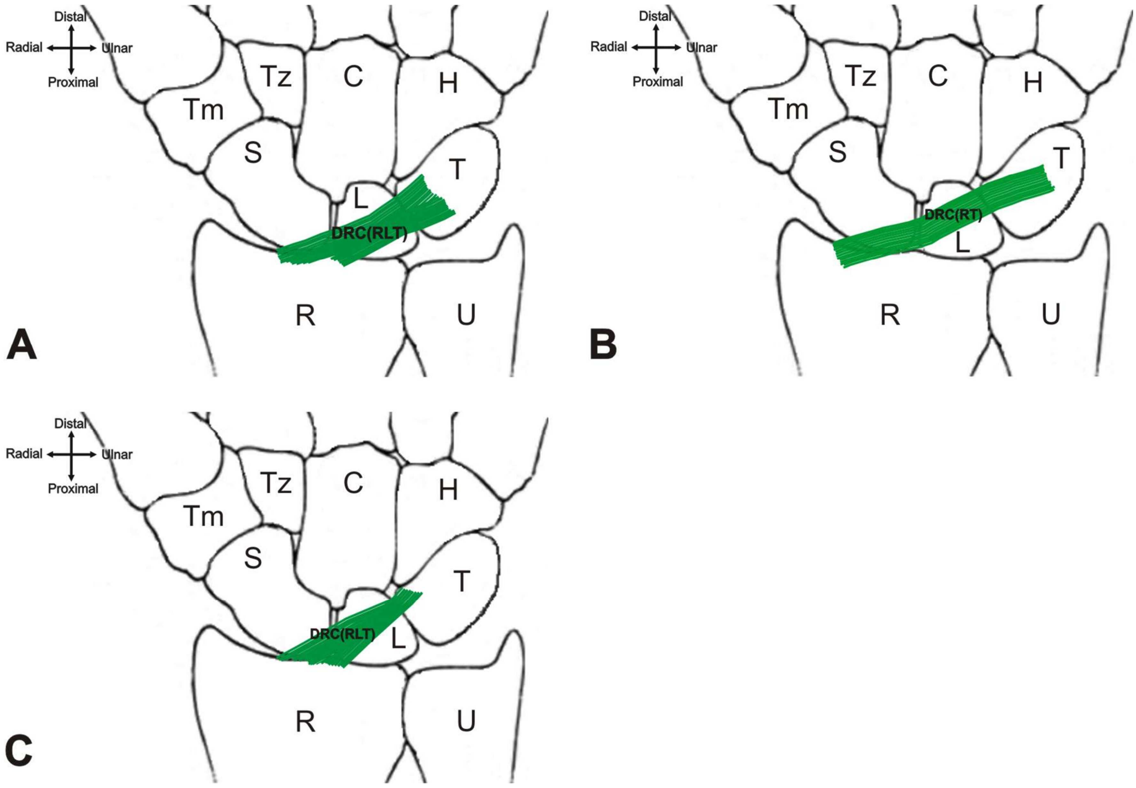

Figure 2. Variable pattern of the dorsal radiocarpal ligament (DRC) reported in the literature. **A.** By Mayfield *et al.* (1976). **B.** By Theumann *et al.* (2003). **C.** By Nagao *et al.* (2005).Rt= Radiotriquetral ligament, RLT= radiolunotriquetral ligament R= radius, U= ulna, S= scaphoid, L= lunate, T= triquetrum, Tm= trapezium, Tz= trapezoid, C= Capitate and H= hamate.

2.1. Dorsal radiocarpal ligament

The DRC is also reported in the literature as the radiotriquetral ligament (RT) and the radiolunotriquertral ligament (RLT) (Feipel and Rooze, 1999; Viegas *et al.*, 1999; Viegas, 2001). Its proximal and distal attachments were consistently described to be on the dorsal aspect of the radius and the dorsal tubercle of the triquetrum respectively (Figure 2) (Mayfield *et al.*, 1976; Berger, 1997; Feipel and Rooze, 1999; Viegas *et al.*, 1999; Berger, 2001; Viegas, 2001; Theumann *et al.*, 2003; Nagao *et al.*, 2005; Nanno and Viegas, 2009). It was reported that the DRC attached to the lunate and fused with lunotriquetral ligamentous fibres as well (Berger, 1997; Berger, 2001). Conversely, it has been demonstrated that the DRC has no bony attachment while extending over the dorsal aspect of the lunate (Figure 2B) (Theumann *et al.*, 2003).

The DRC ligament was classified into four subtypes according to the gross appearance (Mizuseki and Ikuta, 1989). That classification was modified by a later study (Viegas *et al.*, 1999). While a similar description was reported regarding type I and type IV, Type II and type III DRC were found to be different to a lesser extent (Figure 3).

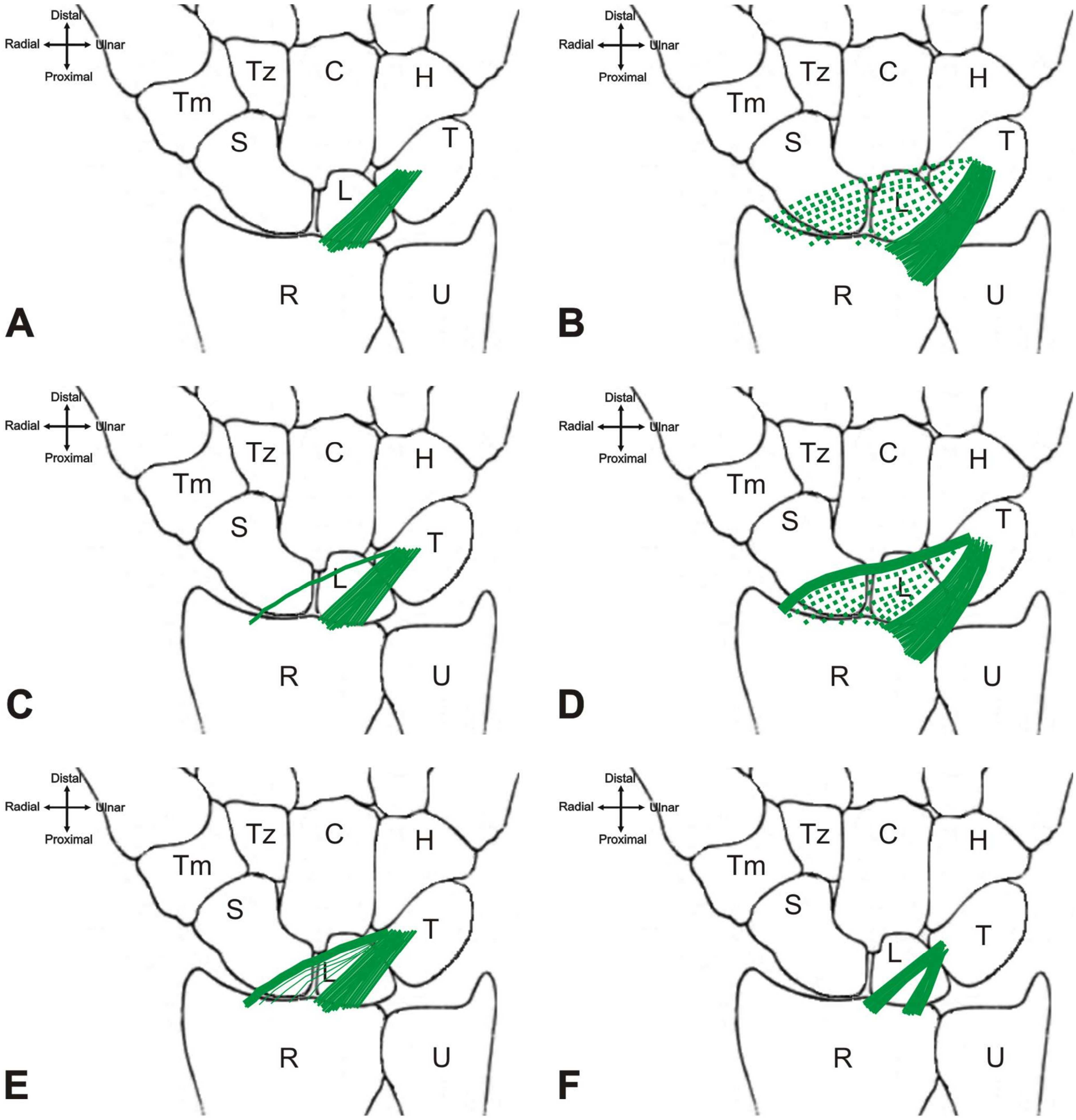

Figure 3. The dorsal radiocarpal ligament (DRC) classification. **A.** Type I extends between the distal ulnar side of the dorsal aspect of the radius and the dorsal tubercle of the triquetrum (Mizuseki and Ikuta,1989; Viegas *et al.*,1999). **B.** Type II; type I with deltoid-shaped thin fibres covering the scaphoid and tapering towards the triquetrum (Mizuseki and Ikuta, 1989). **C.**Type II; type I with extra ligamentous fibres branching between the dorsal tubercle of the triquetrum and the dorsal aspect of the radius (Viegas *et al.*, 1999). **D.** Type III; type II configuration in addition to a thickened part of the radio-distal end of the deltoid fibres (Mizuseki and Ikuta, 1989). **E.** Type III; type II structure with extra fibres extending between the main ligament and its branch (Viegas *et al.*, 1999). **F.** Type IV; type I structure with some ligamentous fibres running from the ulnar side of the radius (Mizuseki and Ikuta, 1989; Viegas *et al.*, 1999). R= radius, U= ulna, S= scaphoid, L= lunate, T= triquetrum, Tm= trapezium, Tz= trapezoid, C= Capitate and H= hamate.

Furthermore, the ligament configuration was investigated and described to have superficial and deep parts. The superficial ulnar part runs from the distal interosseous border of the radius obliquely and ulnarly to the lunate and triquetrum. Similarly, the deep radial part of the ligament runs ulnarly from the posterior border of the radius almost horizontally to terminate on the lunate and triquetrum (Shaaban and Lees, 2006).

3. Radial collateral ligament:

The RCL was reported to consist of broad and thin ligamentous fibres extending from the dorsal aspect of the radial styloid process to the distal tubercle of the scaphoid. It was reported to course distally to blend with the scaphoid- trapezium ligaments. Palmarly, the ligament fused with the sheath contained the flexor carpi radialis tendon and extended deeply to blend with the palmar transverse carpal ligament (Mizuseki and Ikuta, 1989). Also, it was suggested that the ligamentous fibres of the RSC on the distal-most part of the radial styloid process extend towards the waist of the scaphoid to form the RCL (Figure 1B) (Berger and Landsmeer, 1990). Conversely, failure to isolate RCL as a discrete ligament has been reported in the literature (Feipel and Rooze, 1999).

Carpal Instability:

The only tendinous insertion into the carpus is the flexor carpi ulnaris tendon that is inserted into the pisiform bone. As a result, passive forces, joint surface structure, load and ligaments determine carpal motion. A comprehensive understanding of the ligamentous anatomy of the wrist is crucial to better understanding carpal instability. This is further complicated by the complex anatomy, kinematics and patterns of injury (Carlsen and Shin, 2008).

Four groups of carpal instability were discussed in the literature (Linscheid *et al.*, 2002; Trail *et al.*, 2007). Dorsal intercalated segment instability (DISI), palmar intercalated segment instability (PISI), ulnar translocation and dorsal subluxation. While the dorsal extension of the lunate indicates DISI, its volar tipping indicates PISI (Carlsen and Shin, 2008).

The concept of static and dynamic instability was reported. Static instability describes an end state of the condition with manifestation of scapholunate dissociation, fixed flexion of the scaphoid and fixed flexion of the lunate. Partial ligament injury represents dynamic instability with pain and normal or minimally-changed radiographs (Taleisnik, 1984).

Further classification of carpal instability to carpal instability dissociative (CID), carpal instability non-dissociative (CIND), carpal instability complex (CIC) and adaptive carpus were also described in the literature (Dobyns and Gabel, 1990; Trail *et al.*, 2007; Carlsen and Shin, 2008).

A profound knowledge about the ligamentous anatomy of the wrist is essential for proper assessment, management and prevention of the various patterns of carpal instabilities (Palmer *et al.*, 1978; Reagan *et al.*, 1984; Wiesner *et al.*, 1996; Short *et al.*, 2005; Trail *et al.*, 2007; Carlsen and Shin, 2008).

The current study aims to study the variable patterns of the radiocarpal ligaments for three main purposes. First, evaluating the potential variability between the methods of measurement. Second, identifying the best measurement technique in order to limit the variability between different studies and to facilitate comparison. Third, quantifying the size, shape and attachment area of radiocarpal ligaments. For a better understanding of carpal instability, this study should be complemented with further investigation of carpal biomechanics.

Materials and Methods

Ten (n=10) embalmed adult cadaveric upper limbs (3 males and 7 females, 4 right and 6 left hands) without any history of disease or trauma to the wrist were examined at the Laboratory of Human Anatomy, University of Glasgow. Their ages ranged at death from 68 to 93 years (mean age was 86.2 years). The anatomical arrangement of the ligaments attached to the distal radius was studied using gross dissection, micro-dissection and 3D reconstruction.

1. Dissection:

1.1 Description:

The hands and wrists of embalmed cadavers were dissected, both palmarly and dorsally, at the distal third of the forearm up to the carpometacarpal joints. The skin, muscles and flexor and extensor retinacula were carefully excised to avoid damaging the underlying structures. Upon reaching the joint capsule, micro-dissection was done with the strict criteria of tracing individual ligamentous fascicles along their entire length from one attachment to another and excising non-fascicular tissue (under 6X magnification). The periosteum was separated from the radius, ulna and carpal bones to reveal the actual sites of ligamentous attachment.

A single Kirschner wire (K-wire) was drilled through the long axis of the radius and the carpus in order to fix the wrist in the neutral position. Subsequently, each specimen was fixed by two K-wires running through the head of the radius and the third metacarpal bone to firmly fix the specimen on a wooden sheet for 3D reconstruction. A digital microscribe (Immersion Corp., USA) and 3D surface reconstruction software (Rhinoceros 4.0, Robert McNeil & Associates, USA) were used to digitise each ligamentous structure (Figure 4). A rough reconstruction of the underlying bones was performed for reference. The result was a reconstructive image of the wrist bones with the attaching ligaments (Figure 5).

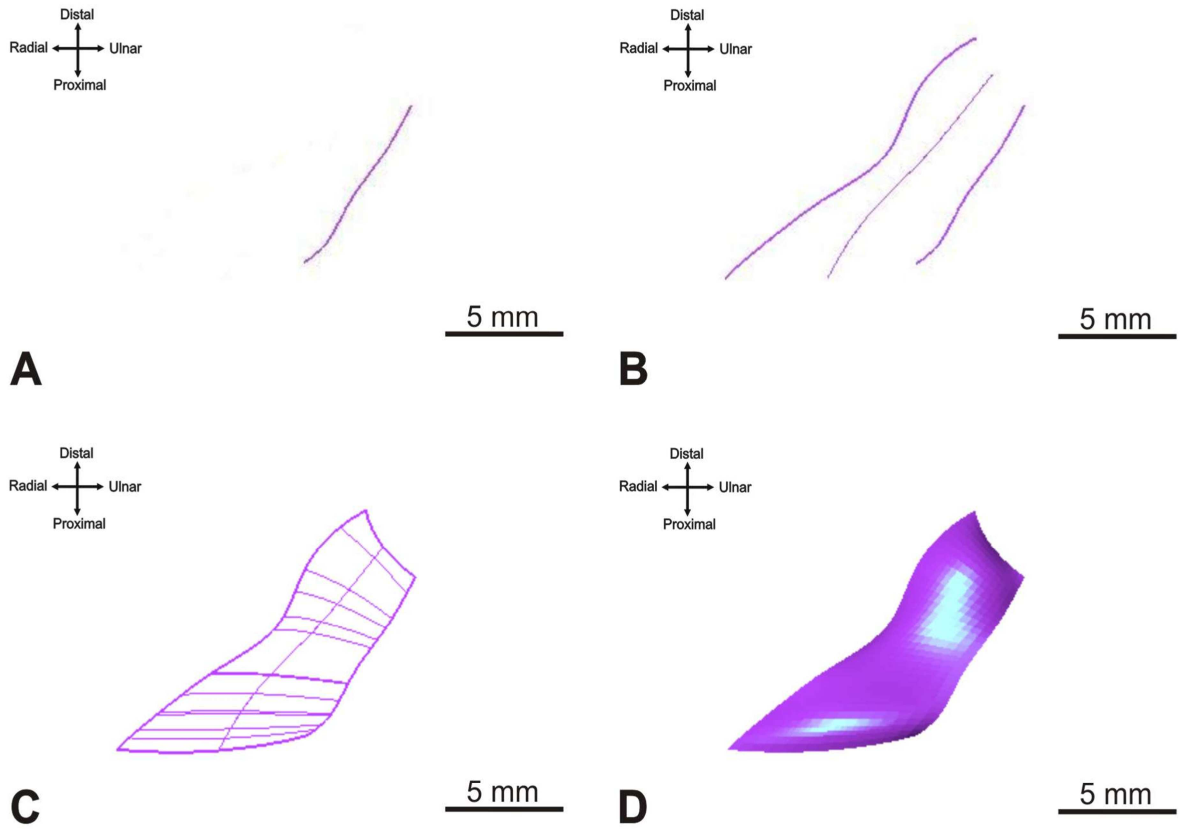

Figure 4. Steps of 3D ligament reconstruction. **A.** A microscribe digitiser was used to trace the most ulnar ligamentous fascicle. **B.** Most ulnar, middle and most radial fascicles were traced ending up with 3 longitudinal dimensions of the ligament. **C.** Lofting of the reconstructed ligamentous surface. **D.** Rendering of the reconstructed surface to reveal the 3D model of the ligament.

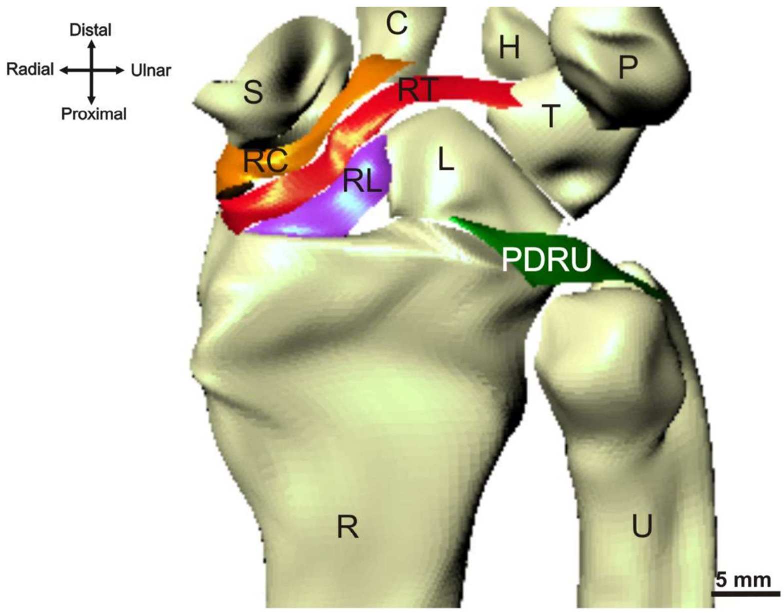

Figure 5. 3D reconstruction of the palmar radiocarpal ligaments. Microscribe reconstruction of the wrist bones together with the radiocapitate ligament (RC), radiotriquetral ligament (RT), radiolunate ligament (RL) and the palmar distal radioulnar ligament (PDRU). R=radius, U=ulna, S= scaphoid, L=lunate, T= triquetrum, P=pisiform, C= Capitate, H= hamate and RL=radiolunate ligament.

For the purpose of studying the area of ligamentous attachments, each ligament was bisected and a careful dissection of the periosteum on each bone was performed to reveal the footprints of each individual ligament. Then, each ligamentous stump was marked with an oil-based marker and reconstructed digitally. Colour-coded ligamentous attachments were created in order to distinguish each ligament while measuring the surface area (Figure 6).

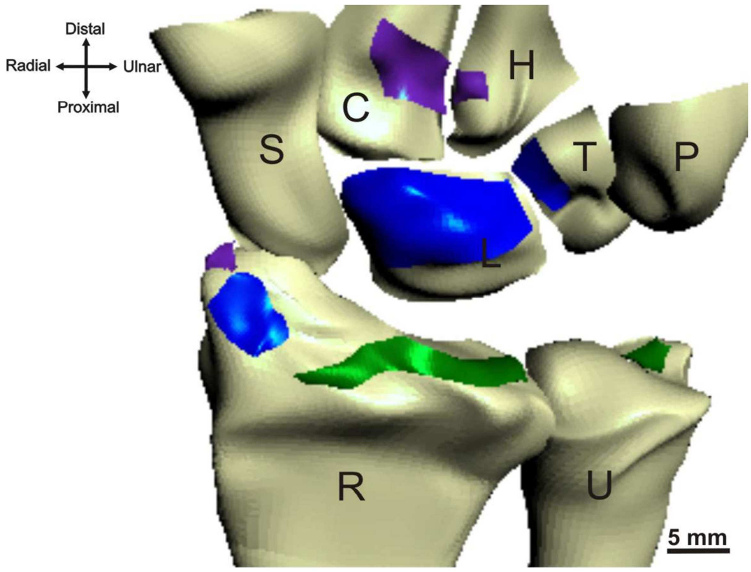

Figure 6. Microscribe reconstruction of the palmar surface of the bony wrist together with the footprints of the radiocapitate-hamate ligament (RC-H) in purple, radiolunotriquetral ligament (RLT) in blue and palmar distal radioulnar ligament (PDRU) in green. R=radius, U=ulna, S= scaphoid, L=lunate, T= triquetrum, P=pisiform, C= Capitate, H= hamate and RL=radiolunate ligament.

1.2 Measurement:

The length (radial [Lr], middle [Lm] and ulnar [Lu]) and width (proximal [Wp], middle [Wm] and distal [Wd]) of each ligament around the distal radius were measured manually using standard callipers (Figure 7). Then, specimens were photographed with a digital camera (Canon EOS 40D) under studio lighting. Using Image J 1.44 software, the length and width were measured digitally (Figure 8).

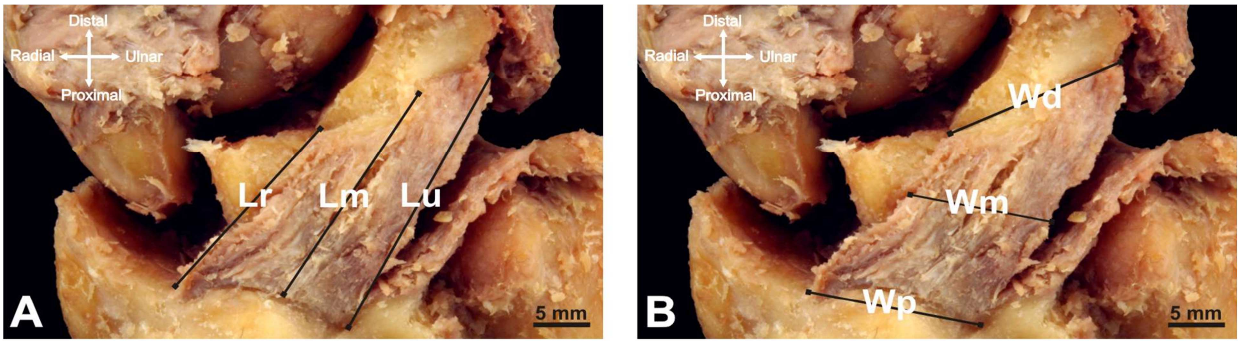

Figure 7. Dimensions of manual measurement of the dorsal radiocarpal ligament (DRC). **A.** A calliper was used to measure the ligamentous length at three levels: radial (Lr), middle (Lm) and ulnar (Lu) of each ligament. **B.** Ligamentous width at the proximal (Wp), middle (Wm) and distal (Wd) aspects of the ligament.

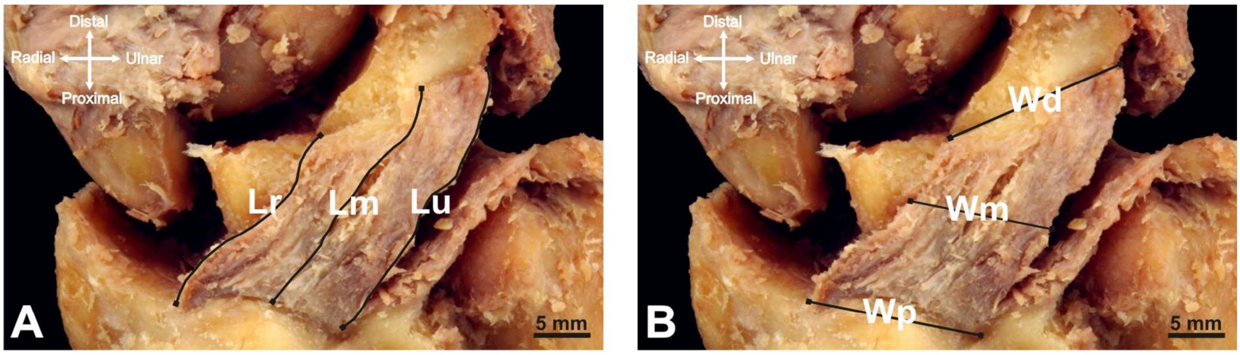

Figure 8. Parameters of the digital measurement of the dorsal radiocarpal ligament (DRC). **A.** A segmented line tool of Image J was used to trace the entire fascicle running on the various aspects of each ligamentous length; radial (Lr), middle (Lm) and ulnar (Lu). **B.** Width was measured with similar technique of the manual measurement but digitally. Width measurement includes proximal (Wp), middle (Wm) and distal (Wd) levels. Note: this technique was also used to measure the ligamentous dimensions with a microscribe digitiser.

The length, width at three levels and surface area of each ligament were measured from the reconstructed 3D model with 3D surface reconstruction software (Rhinoceros 4.0, Robert McNeil & Associates, USA) (Figure 8).

The length and width measurements of all the ligaments attached to the distal radius were documented twice for each ligament per method of measurement by the same observer (R.A.). Also, the total ligament surface areas as well as the ligamentous attachment area were calculated using the microscribe method.

1.2.1 Planar and non-planar ligaments:

In order to determine the variability among the three included methods of measurement, ligaments were arranged in two groups based on their shape and the plane they occupied; planar and multi-planar ligaments. Planar ligaments consist of fascicles running straight from one attachment to another in the same plane. Multi-planar ligaments are truly three-dimensional; they would curve out of any single planar section. A comparative statistical analysis was done with a t-test assuming two unequal variants with 95% accuracy ($P < 0.05$). For multiple rounds of measurement with each technique, this determined the accuracy of each technique for each type of ligament.

1.2.2 Specific ligaments:

Consistent descriptive terms were used to name each ligament in a way that reflects their bony attachments. As a result, some analogous terms in the cited references were inevitably replaced.

The attachments and course of each ligament were determined in addition to the morphometric description. A t-test assuming two unequal variants was done when functionally important variability was suspected. $P<0.05$ was considered to be statistically significant.

2. Histological Preparation:

The DRC (RT), PDRU, RSC and RLT were arbitrarily selected to study their actual ligamentous attachments (entheses) histologically. Each ligament was excised together with the attached bones to study the actual attachment of the ligamentous fibres. A small K-wire was drilled through all the attached bones to each ligament in order to firmly fix the ligament throughout the tissue preparation. The specimens were processed and stained using a modified Masson’s Trichrome technique (Appendix 1).

After histological preparation, each slide was photographed; stitching multiple overlapped images that were taken under 2.5 x magnifications created a panorama image. The area [A], perimeter [P] and length [L] of individual ligamentous attachments over each bone together with capsular (non-ligamentous) attachment were measured using Image J 1.44.

In order to account for variable attachment lengths, the mean index A (Area/Length) and P (Perimeter/Length) of each histological ligamentous attachment was calculated. Subsequently, the mean and standard deviation were reported.

Results

1. Quantitative Analysis:

Various configurations of ligamentous connections of the distal radius to the carpus, TFCC and ulna have been identified. According to their morphological variability and bony attachments, the sample population could be divided into subgroups.

1.1. Planar and Multi-planar Ligaments:

Among all the radiocarpal ligamentous connections of the studied sample, three connections were identified with a planar configuration whereas twelve connections showed a multi-planar pattern (Table 1).

Radiocarpal Ligament configuration	
Planar Ligaments	**Multi-planar Ligaments**
Radiolunate ligament (RL) Long radiolunate ligament (LRL) Short radiolunate ligament (SRL)	Radiocapitate ligament (RC) Radioscaphocapitate ligament (RSC) Radioscaphocapitate ligament with a triquetral band (RSC-T) Radiolunotriquetral ligament (RLT) Radiotriquetral ligament (RT) Radioradial ligament (RR) Rradioscaphoid ligament (RS) Palmar/dorsal radio-triangular fibrocartilage complex ligament (R-TFCC) Dorsal radiocarpal ligament (DRC) Palmar distal radioulnal ligament (PDRU) Dorsal distal radioulnar ligament (DDRU)

Table 1. Planar and multi-planar radiocarpal ligaments.

Based on the results of the three methods of measurement (Table 2), there were minor differences between planar ligament measurements. Measurement of the multi-planar ligaments showed an increase in the length with digital method in comparison to the manual method, whereas microscribe length and width measurements were increased compared with the manual and digital methods.

	Mean Length (mm)			Mean Width (mm)		
	Lr	Lm	Lu	Wp	Wm	Wd
Planar Ligaments						
Manual	13.8 ± 7.5	13.5 ± 6.2	11.6 ± 5.4	7.7 ± 2.9	7.1 ± 1.9	8.1 ± 2.2
Digital	11.3 ± 7.2	13.3 ± 6.3	11.4 ± 6.0	7.4 ± 3.3	7.1 ± 2.3	7.5 ± 2.1
Microscribe	13.8 ± 7.3	14.6 ± 7.2	12.5 ± 6.0	8.2 ± 3.7	6.7 ± 2.5	7.6 ± 2.7
Multi-planar Ligaments						
Manual	18.5 ± 9.9	19.2 ±10.1	18.8 ± 10.3	10.8 ± 8.9	9.3 ± 9.1	10.6 ± 9.0
Digital	19.4 ± 11.0	20.4 ± 11.3	20.4 ± 11.9	10.6 ± 9.2	9.1 ± 9.1	11.0 ± 10.1
Microscribe	21.8 ± 12.1	21.6 ± 12.0	210 ± 12.3	11.4 ± 10.1	10.1± 10.4	11.8 ± 10.9

Table 2. Mean ligament dimensions (± standard deviation) of the planar and multi-planar ligaments with manual, digital and microscribe methods. Lr=radial length, Lm= middle length, Lu= ulnar length, Wp= proximal width, Wm= middle width and Wd= distal width.

1.2. Measurements:

All ligaments were measured twice at different times using manual, digital and microscribe methods. There were significant differences ($p < 0.05$) between ligament dimensions in relation to the method of measurement and the morphology of the ligaments. In the case of planar ligaments such as the RL, there were no significant differences ($p > 0.05$) between the rounds of measurement with all three methods (Figure 9). Conversely, significant difference ($p < 0.05$) was observed with manual and digital rounds of measurement of multi-planar ligaments such as the PDRU at different levels; but microscribe rounds of measurement remained consistent (Figure 10). For the remainder of this thesis, only microscribe measurements will be reported (Table 3).

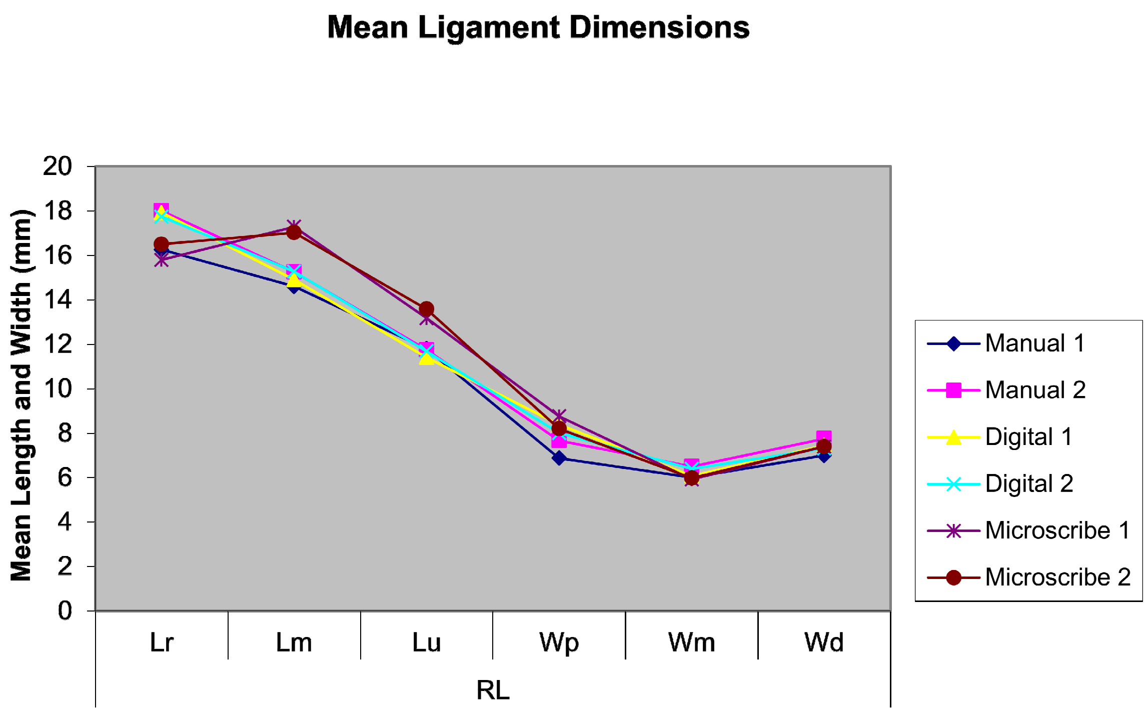

Figure 9. Mean ligament dimensions of a planar ligament, the radiolunate ligament (RL), through the rounds of measurement with manual, digital and microscribe methods. Lr=radial length, Lm= middle length, Lu= ulnar length, Wp= proximal width, Wm= middle width and Wd= distal width.

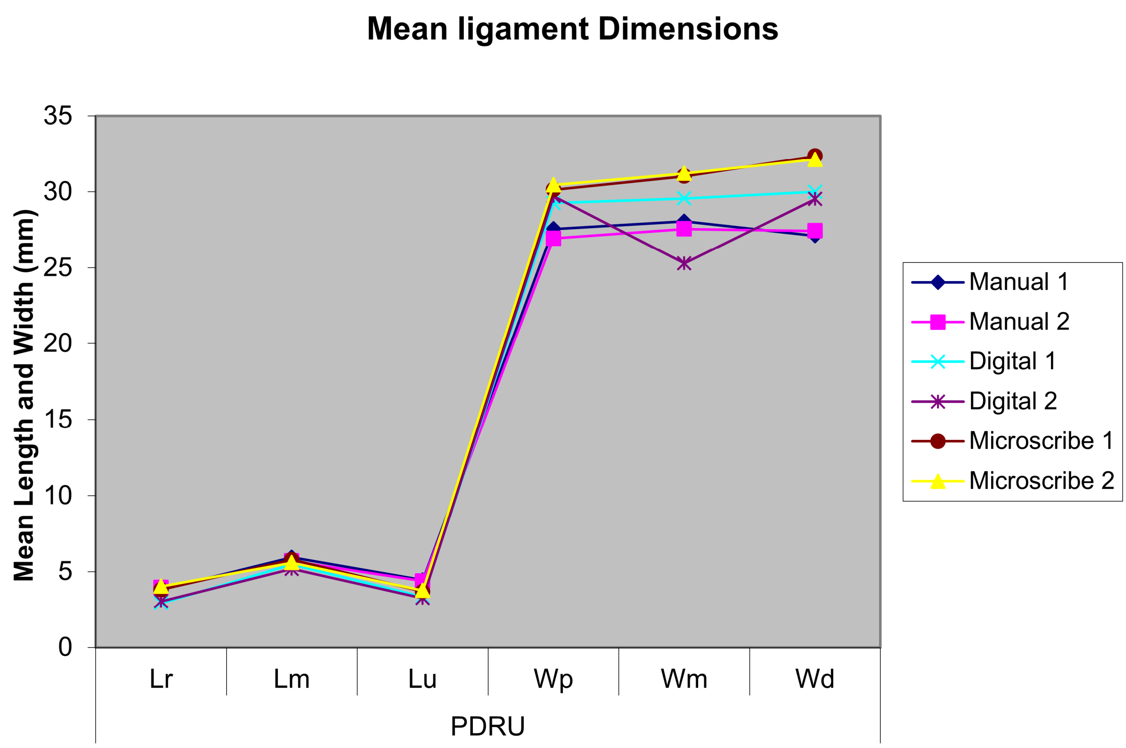

Figure 10. Mean ligaments dimension of a multi-planar ligament, the palmar distal radioulnar ligament (PDRU), through the rounds of measurement with manual, digital and microscribe methods. Lr= radial length, Lm= middle length, Lu= ulnar length, Wp= proximal width, Wm= middle width and Wd= distal width.

	Mean Length (mm)			Mean Width (mm)		
	Lr	Lm	Lr	Wp	Wm	Wd
Palmar Ligaments						
RC	27.3 ± 2.4	28.9 ± 4.7	31.0 ± 3.8	4.9 ± 1.0	2.8 ± 1.5	8.2 ± 2.8
RSC	33.0 ± 5.4	31.4 ± 3.9	31.2 ± 3.0	3.5 ± 2.1	4.5 ± 2.4	5.1 ± 1.3
RSC-T	30.5 ± 2.2	33.4 ± 3.5	37.1 ± 3.5	10.1 ± 0.8	7.0 ± 1.4	17.8 ± 2.2
RL	16.1 ± 2.5	17.2 ± 3.0	13.4 ± 2.8	8.5 ± 3.7	6.0 ± 1.7	7.4 ± 2.4
LRL	22.8 ± 1.0	22.8 ± 0.7	21.0 ± 1.0	8.1 ± 4.6	8.2 ± 0.3	9.5 ± 0.3
SRL	4.0 ± 0.4	4.8 ± 0.9	5.3 ± 0.8	7.9 ± 3.4	7.0 ± 3.8	6.8 ± 3.8
RLT	33.4 ± 2.6	34.0 ± 3.3	30.0 ± 5.0	6.2 ± 3.2	6.2 ± 2.7	5.4 ± 2.8
RT	35.1 ± 2.2	34.4 ± 3.2	33.5 ± 4.0	6.8 ± 3.8	4.5 ± 2.8	4.3 ± 0.9
RS	21.0 ± 7.6	22.2 ± 7.4	21.5 ± 7.8	3.5 ± 0.3	3.1 ± 0.7	3.9 ± 0.5
RR	2.6	1. 5	3.3	24.9	25.1	26.6
PDRU	3.9 ± 1.9	5.7 ± 2.3	3.7 ± 1.1	30.3 ± 8.8	31.1 ± 8.1	32.2 ± 6.9
R-TFCC*	---------	----------	-----------	4.5	4.0	-----------
Dorsal ligaments						
DRC (RLT)	27.7 ± 6.5	26.2 ± 4.3	25.8 ± 2.7	9.7 ± 6.4	7.1 ± 2.9	6.7 ± 4.4
DRC(RT)	26.7 ± 4.7	24.7 ± 4.7	24.0 ± 5.4	5.2 ± 2.9	3.3 ± 1.0	3.1±1.0
DDRU	5.8 ± 4.3	3.5 ± 1.1	3.7 ± 1.1	16.3 ± 0.8	15.4 ± 2.2	15.3 ± 3.7
R-TDFCC	13.0±1.2	11.6±2.6	10.6±3.3	6.3±3.2	4.0±0.4	4.5±0.9

*The palmar R-TFCC was continuous with the dorsal R-TFCC so the measurements were restricted on the WP and Wm.

Table 3. Mean ligament dimensions (± standard deviation) of the palmar and dorsal radiocarpal ligaments obtained with the microscribe digitiser (3D reconstruction) method. Lr= radial length, Lm= middle length, Lu= ulnar length, Wp= proximal width, Wm= middle width and Wd= distal width.

2. Anatomy of Specific Radiocarpal ligaments:

2.1. Palmar radiocarpal ligaments:

Twelve different modes of connection between the palmar aspects of the distal radius to the carpal bones were identified. Radiocapitate ligament (RC) (Figure 11B), radiolunotriquetral ligament (RLT) (Figure 11A & C), radioscaphocapitate ligament (RSC) (Figure 11A & C), radioscaphocapitate ligament with a triquetral band with or without a hamate attachment (RSC-T/ RSC-TH) (Figure 11A & D), radiolunate ligament (RL) (Figure 11B & C), long radiolunate ligament (LRL) (Figure 11A & D), short radiolunate ligament (SRL) (Figure 11A & D), radiotriquetral ligament (RT) (Figure 11B & C), radioradial ligament (RR), radioscaphoid ligament (RS) (Figure 11C & D), palmar distal radioulnar ligament (PDRU) (Figure 11A,B & D) and radio-triangular fibrocartilage complex ligament (R-TFCC) (Figure 11C) were reported as distinguishable structures in this study.

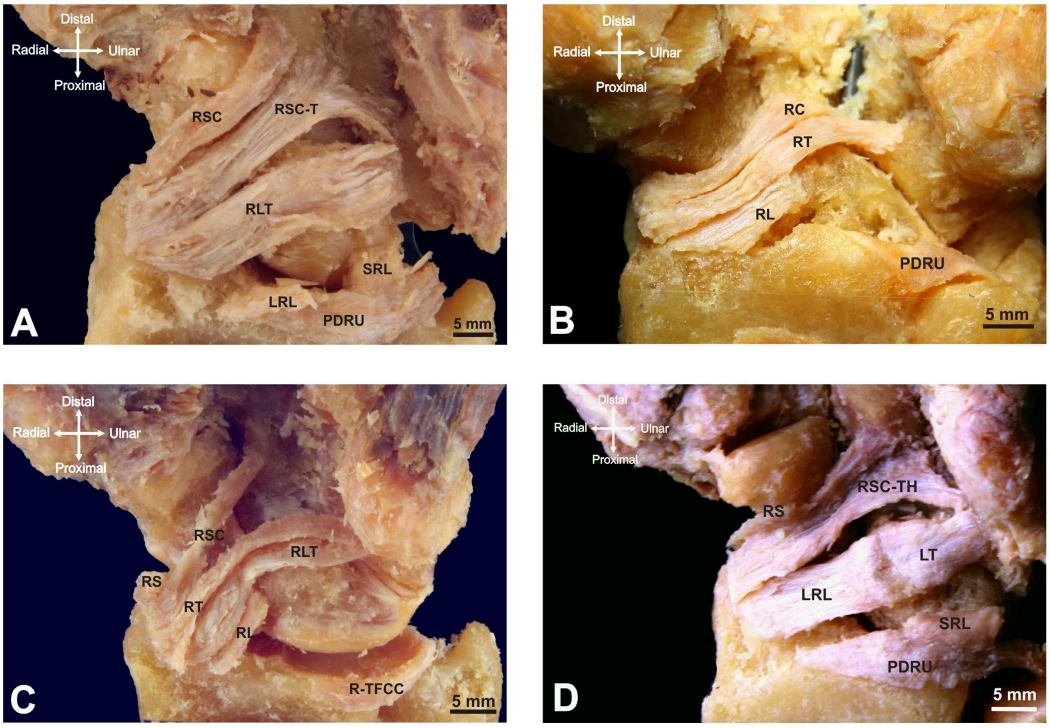

Figure 11. Various palmar radiocarpal ligaments. RC=radiocapitate ligament, RLT= radiolunotriquetral ligament, RSC= radioscaphocapitate ligament, RSC-T= radioscaphocapitate ligament with a triquetral band, RSC-TH= radioscaphocapitate ligament with triquetrum and hamate attachments, RL= radiolunate ligament, LRL= long radiolunate ligament, SRL= short radiolunate ligament, RT= radiotriquetral ligament, RS= radioscaphoid ligament, PDRU= palmar distal radioulnar ligament and R-TFCC= radio-triangular fibrocartilage complex ligament.

2.1.1. Radiocapitate Connections:

The connection between the distal radius and the capitate was represented by three different modes. It is either a simple connection between the styloid process of the radius and the central and palmar aspect of the capitate forming a RC (n=2; 20%) (Figure 12) or a more complex link between the radial styloid process, scaphoid fossa and the body of the capitate in the form of a RSC (n=3; 30%). The RSC was often attached to the triquetrum by a ligamentous band branching from the main ligament towards the palmar and radial aspect of the triquetrum, and was designated RSC-T (n=5; 50%). The proximal attachment of the RSC and RSC-T was found to partially overlap the proximal attachment of the radiolunate ligaments (Figure 13).

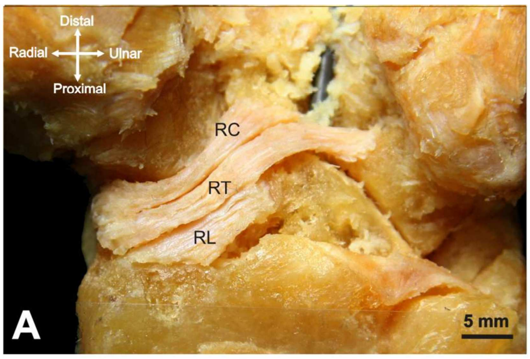

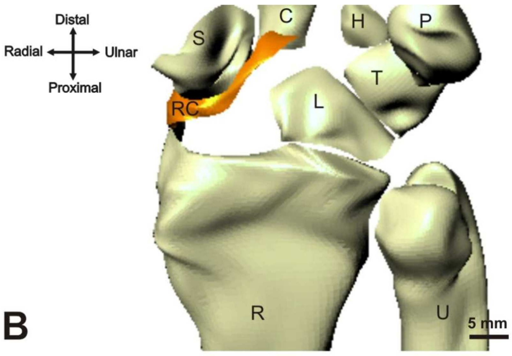

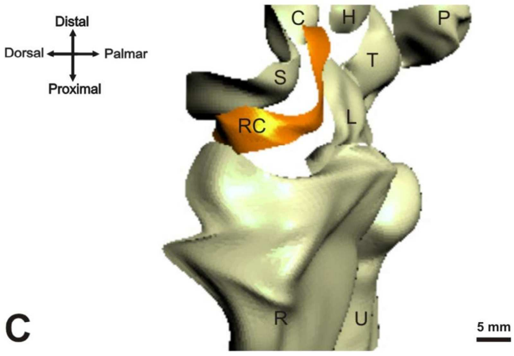

Figure 12. The radiocapitate ligament (RC). **A.** The RC is connecting the radial styloid process to the body of the capitate and running adjacent to the radiotriquetral ligament (RT). **B.** Microscribe reconstruction of the same specimen (palmar view). **C.** Another view of the same specimen showing the actual radial attachment of the RC.R=radius, U=ulna, S= scaphoid, L=lunate, T= triquetrum, P=pisiform, C= Capitate, H= hamate and RL= radiolunate ligament.

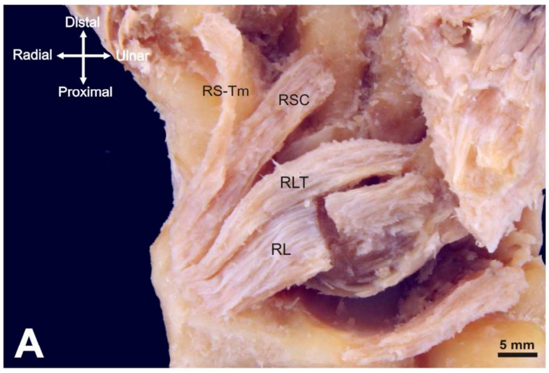

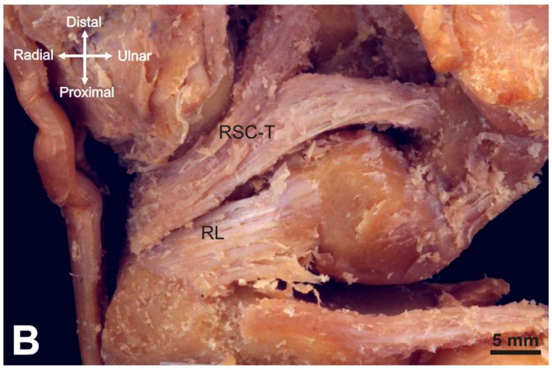

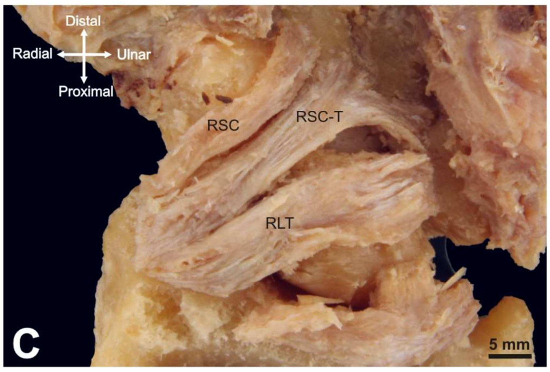

Figure 13. The radioscaphocapitate ligament (RSC) variations. **A.** RSC without a triquetrum attachment, ulnar to the radioscaphotrapezium ligament (RS-Tm) and radial to the radiolunotriquetral ligament (RLT). **B.** RSC with a triquetrum connection (RSC-T) by a secondary branch from the main ligament; proximally overlaps the radiolunate ligament (RL). **C.** RSC together with RSC-T. Unlike in (A), RSC is the radial-most palmar radiocarpal ligaments.

The RSC-T had a significantly greater mean Lu (37.1 ± 3.5 mm) than that of the RSC (31.2 ± 3.0 mm; $p<0.05$; Table 3). Also, the RSC-T had significantly wider mean Wp (10.1 ± 0.8 mm) and Wd (17.8 ± 2.2 mm) in comparison with the RSC mean Wp (3.5 ± 2.1mm) and (5.1 ± 1.3 mm; $p<0.05$; Table 3).

The RSC had significantly smaller mean surface area (126.7 ± 44.1 mm^2) than the RSC-T (287.0 ± 24.45 mm^2; $p<0.05$) but there was no significant difference between the mean surface area of the RSC and the RC (116.9 ± 52.5 mm^2; $p>0.05$). Also, the mean surface area of the RC was significantly smaller than that of RSC-T ($p<0.05$) (Table 4).

Mean surface area of radiocarpal ligaments (mm^2)	
Palmar Ligaments	
RC	116.9 ± 52.5
RSC	126.7 ± 44.1
RSC-T	287.0 ± 24.45
RL	97.3 ± 43.7
LRL	191.98 ± 12.0
SRL	29.5 ± 13.4
RLT	191.0 ± 100.4
RT	164.9 ± 98.9
RS	61.7 ± 23.8
RR	51.2 ± 51.2
PDRU	137.0 ± 56.2
R-TFCC	It was continuous with the dorsal R-TFCC ligament
Dorsal ligaments	
DRC (RLT)	159.6 ± 83.2
DRC (RT)	79.8 ± 33.7
DDRU	55.2 ± 17.5
R-TDFCC	45.6 ± 11.1

Table 4. Mean surface area (± standard deviation) of the palmar and dorsal radiocarpal ligaments obtained with the microscribe digitiser (3D reconstruction) method.

When considering the individual ligament attachment to each bone, the mean proximal attachment area of the RSC-T (15.54 ± 5.43 mm^2) was significantly greater than that of the RSC ligament (6.88 ±0.63 mm^2) as well as the RC (7.07 .15 mm^2, $p<0.05$) (Table 5).

Ligaments	Location	Area (mm2)	Specimens (N = 10)
Palmar ligaments			
RC (H)	Radius	7.07 ± 0.15	2
	Capitate	38.12 ± 1.38	2
	Hamate*	7.29	1
RSC	Radius	6.88 ± 0.63	3
	Scaphoid	13.84 ± 0.68	3
	Capitate	37.92 ± 1.31	3
RSC-T (H)	Radius	15.54 ± 5.43	5
	Scaphoid	18.05 ± 6.12	5
	Capitate	34.14 ± 14.82	5
	Triquetrum	8.02 ± 1.42	5
	Hamate*	8.00	1
RLT	Radius	21.30 ± 16.76	5
	Lunate	71.27 ± 58.69	5
	Triquetrum	14.28 ± 7.76	5
RL	Radius	31.94 ± 5.75	5
	Lunate	31.99 ± 2.08	5
LRL	Radius	42.55 ± 11.24	3
	Lunate	43.88 ± 7.91	3
SRL	Radius	8.90 ± 1.15	3
	Lunate	16.97 ± 4.61	3
RT	Radius	4.70 ± 0.34	3
	Triquetrum	7.42 ± 0.01	3
RR	Radius -lateral	11.88	1
	Radius - medial	6.35	1
RS-Tm	Radius	6.16 ± 1.08	3
	Scaphoid	5.27 ± 0.51	3
	Trapezium*	7.77	1
R-TFCC	Radius	19.56	1
PDRU	Radius	52.75 ± 27.26	8
	Ulna	14.42 ± 9.31	8
Dorsal ligaments			
DRC (RLT)	Radius	18.19 ± 22.20	9
	Lunate	25.31 ± 21.10	9
	Triquetrum	14.98 ± 10.63	9
	Radius		5
(RT)	Triquetrum	16.36 ± 10.91	5
		10.63 ± 6.80	
R-TFCC	Radius	12.68 ± 5.36	5
DDRU	Radius	9.91 ± 5.91	4
	Ulna	8.03 ± 6.18	4

* Minor attachment

Table 5. Mean ligament attachment area (± standard deviation) of the palmar and dorsal radiocarpal ligaments obtained with the microscribe digitiser (3D reconstruction) method.

RC (H)= radiocapitate ligament with or without hamate attachmentt; RSC= radioscaphocapitate ligament; RSC-T (H)= radioscaphocapitate ligament with a triquetral band or with a triquetral band and hamate attachment; RLT= radiolunotriquetral ligament;; RL= radiolunate ligament; LRL= long radiolunate ligament; SRL= short radiolunate ligament; RT= radiotriquetral ligament; RR= radioradial ligament; RS= radioscaphoid ligament; R-TFCC= radio-triangular fibrocartilage complex ligament; PDRU= palmar distal radioulnal ligament; DRC= dorsal radiocarpal ligament; DDRC= dorsal distal radioulnar ligament.

Neither a significant difference between the mean distal attachment areas nor between the scaphoid attachment of the RSC-T and RSC was identified (p>0.05) (Figure 14). An attachment to the hamate was identified both when a RC was present, (n = 1) and when a RSC-T was present (n = 1; Figure 15).

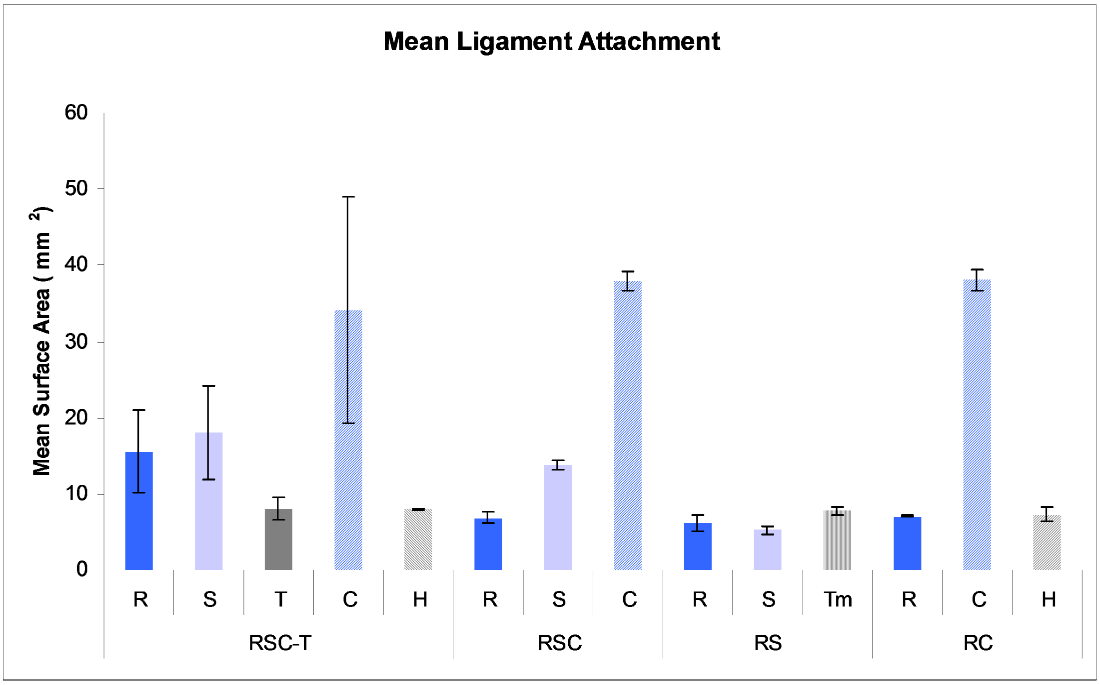

Figure 14. Mean ligament attachments of the radiocapitate and radioscaphoid connections. RSC-T radioscaphocapitate ligament with a triquetral band, RSC=radioscaphocapitate ligament, RS=radioscaphoid ligament, RC, radiuocapitate ligament R=radius, S= scaphoid, C= Capitate, Tm-trapezium and H= hamate, Scale bar= standard deviation.

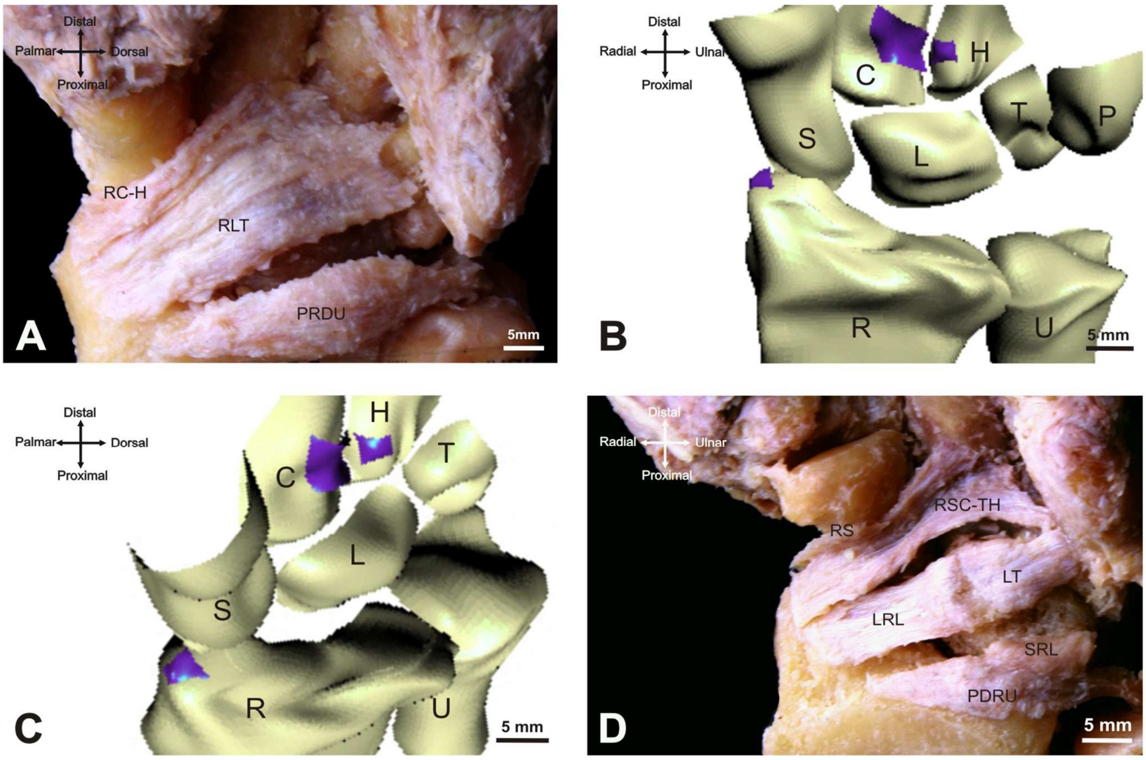

Figure 15. Radiocapitate connection in relation to the hamate. **A.** The Radiocapitate ligament with a distal attachment to the hamate (RC-H). **B.** Miocroscribe reconstruction of the same specimen and view in (A) showing the footprints of the RC-H on the radius(R), capitate (C) and hamate (H). **C.** Another 3D reconstruction view revealing the actual radial attachment of the RC-H. **D.** The radioscaphocabitate ligament with a triquetrum (T) and hamate (H) attachment (RSC-TH) with the radioscaphoid ligament (RS) on its radial proximal border. The radial proximal margin of the long radiolunate ligament (LRL) is partially overlapped by the RSC-TH. U= ulna, S= scaphoid, L= lunate, P= pisiform, PDRU= palmar distal radioulnar ligament and RL= radiolunate ligament.

2.1.2. Radioscaphoid Connections:

A discrete RS (n=3; 30%) was identified to be consistently attached to the radial-most aspect of the wrist between the styloid process of the radius (Figure 16). Quantitative descriptions were obtained (Tables 3, 4 and 5).

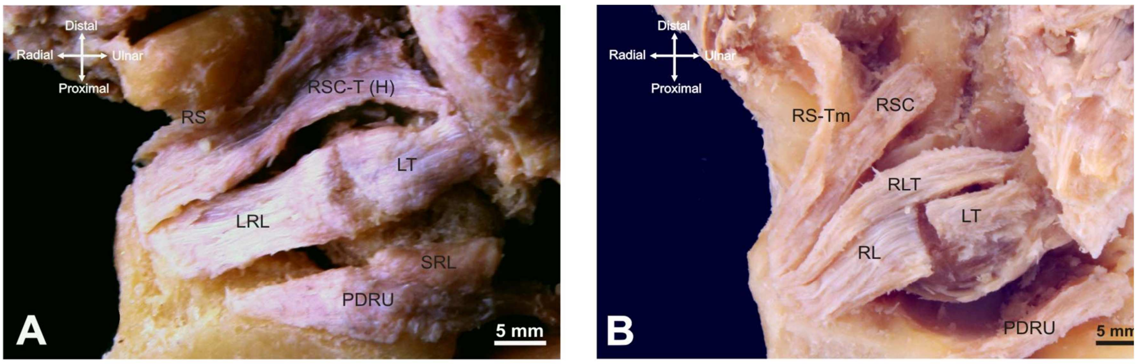

Figure 16. The radioscaphoid ligament (RS). **A**- The RS (no trapezium attachment), the long radiolunate ligament (LRL) seperated from the lunotriquetral ligament (LT) and the short radiolunate (SRL) is proximally overlapped by the palmar dorsal radioulnar ligament (PDRU). **B-** The RS with a trapezium attachment, radioscaphotrapezial ligament (RS-Tm), combined and separated radiolunate ligament (RL) and LT.

In addition to the attachment of the RS to the distal radius and the scaphoid, it may give attachment to the palmar edge of the trapezium as well, forming a radioscaphotrapezial ligament (RS-Tm: n=1; 10%; Figure 16B). Quantitative descriptions for both were obtained (Tables 3, 4 and 5).

2.1.3. Radiolunate Connections:

The ligamentous attachments between the distal radius and the lunate were highly variable. Palmar ligaments may have a single and separate attachment to the lunate by the RL (n=5; 50%) or a double attachment by the LRL (n=3, 30%) and SRL (n=3, 30%). Similar to the RL, the LRL originated from the palmar edge of the scaphoid fossa and runs towards the distal edge of the lunate. Along its course, its proximal attachment was partially overlapped by the RSC. The SRL extends from the ulnar side of the palmar edge of the lunate fossa towards the palmar edge of the lunate (Figure 16). Quantitative descriptions (Tables 3, 4 and 5) demonstrated the distinct differences between these ligamentous types.

The RL fibres may merge with those fibres of the lunotriquetral ligament (LT) so both ligaments become inseparable from each other ending up with RLT (N=5, 50%) formation

(Figure 17). Quantitative descriptions were obtained (Tables 3, 4 and 5).

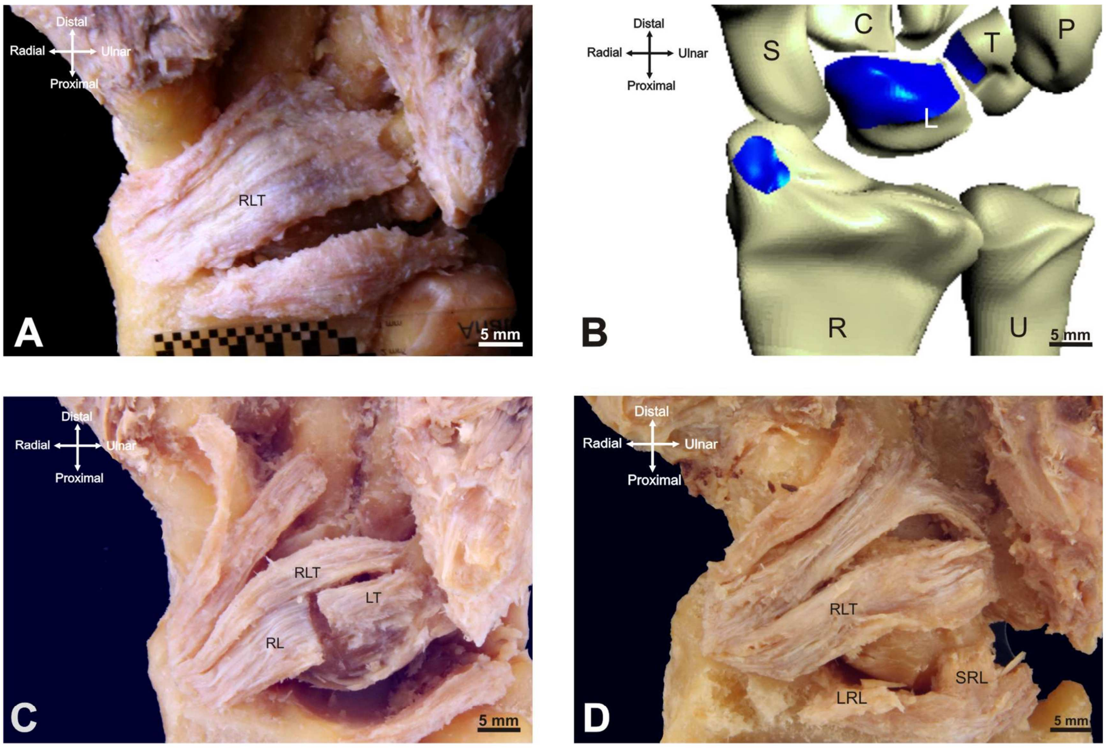

Figure 17. The radiolunotriquetral ligament (RLT) variations. **A.** Wide single RLT. **B.** Microscribe reconstruction of the same specimen in (A) showing the actual ligamentous attachments of the RLT. **C.** Thin RLT and separated radiolunate (RL) and lunotriquetral ligament (LT) **D.** RLT together with long (LRL) and short (SRL) radiolunate ligaments. The distal aspect of the LRL was excised in favour of better SRL view. R= radius, U= ulna, S= scaphoid, L= lunate, T= triquetrum, P= pisiform and C= Capitate.

Another attachment between the distal end of the radius and the triquetrum was found to be a more direct and simple connection between the two bones (Figure 18). The RT (n=3, 30%) was proximally attacheed to the distal radius (4.70 ± 0.34 mm^2) and then coursed distally to the radial-most and palmar aspect of the triquetrum (7.42 ± 0.01 mm^2). No significant differences between the RT and RLT attachments were noticed ($p>0.05$) (Figure 19).

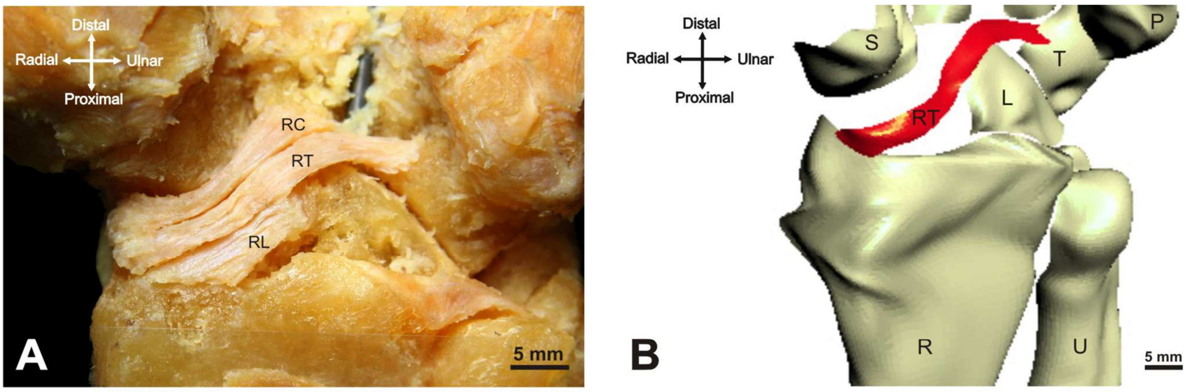

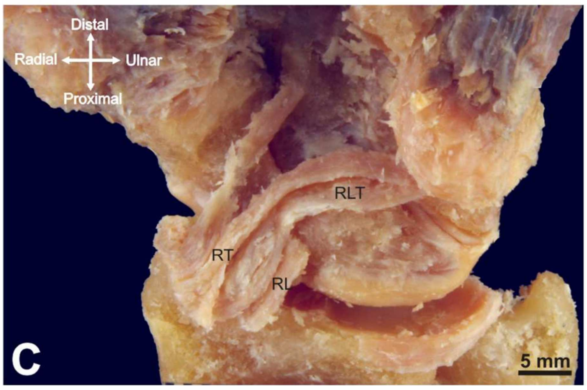

Figure 18. The radiotriquetral ligament (RT) configuration. **A.** RT overlapping the radiolunate ligament (RL). **B.** Microscribe reconstruction of the same specimen in (A) for the RT. **C.** RT together with radiolunotriquetral ligament (RLT) overlapping the RL. RC= radiocapitate ligament, R= radius, U= ulna, S= scaphoid, L= lunate, T= triquetrum and P= pisiform.

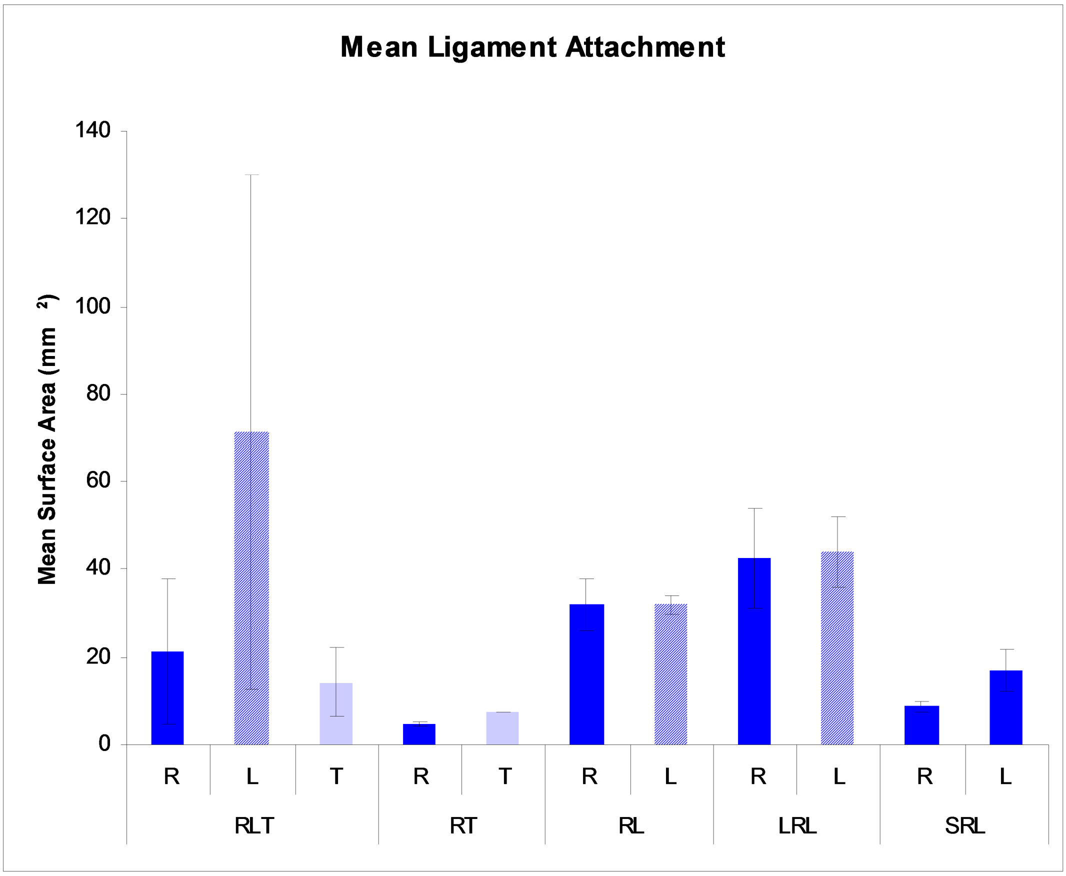

Figure 19. Radiolunate ligaments with their mean osseous attachment areas. RLT=radioluntriquetral ligament, RT=radiotriquetral ligament, RL=radiolunate ligament, LRL=long radiuolunate ligament, SRL=short radiolunate ligament, R=radius, L=lunate and T= triquetrum, Scale bar = standard deviation.

2.1.4. Radioradial Connections:

Fine and thin ligamentous fibres of the RR (n=1; 10%) bridging two separate areas of the distal radius were identified (Figure 20). They were observed to be proximally attached (11.88 mm^2) just ulnar to the LRL attachment and run towards the ulnar end of the radius (6.35 mm^2).

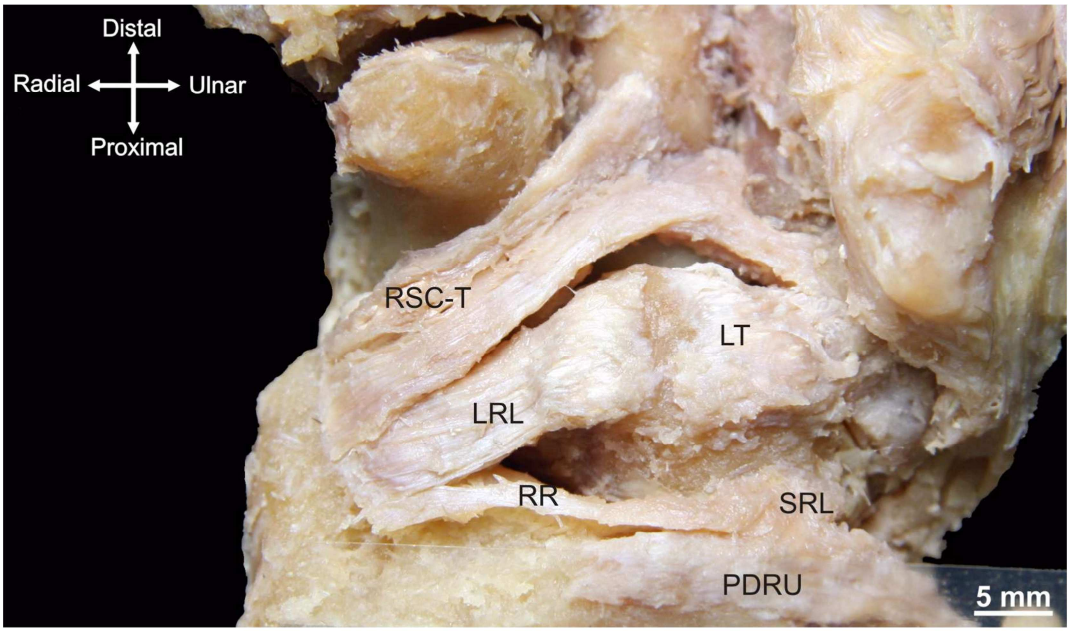

Figure 20. Very proximal radioradial ligament (RR) runs horizontally from the lateral to the medial end of the radius with combined short radiolunate ligament (SRL). RSC-T=radioscaphocapitate ligament with a triquetral attachment, LRL=long radiolunate ligament, Lt= lunotriquetral ligament and PDRU=palmar distal radioulnar ligament.

2.2. Dorsal Radiocarpal Ligaments:

Three distinct radiocarpal ligaments were observed on the dorsal aspect of the wrist. Dorsal radiocarpal ligament (DRC) (Figure 21), radio-triangular fibrocartilage complex ligament (R-TFCC) (Figure 20C) and the dorsal distal radioulnar ligament (DDRU) (Figure 21D) were identified.

Radiotriquetral Connections:

The DRC was found to have such a complex configuration. Two different connections between the dorsal distal aspect of the radius and the triquetrum made the base of the DRC configuration. The first connection was represented by the radiotriquetral band (RT: n=5; 5%), which proximally spanned the area between the ulnar and dorsal portions of the distal end of the radius and the interfossal ridge between the scaphoid and lunate fossae; it was then attached to the proximal and dorsal aspects of the dorsal tubercle of the triquetrum (Figure 21). The radiolunotriquetral band (RLT: n=9; 90%), with the same structure of the radiotriquetral band in addition to its attachment to the lunate, was the second connection (Figure 21B & C).

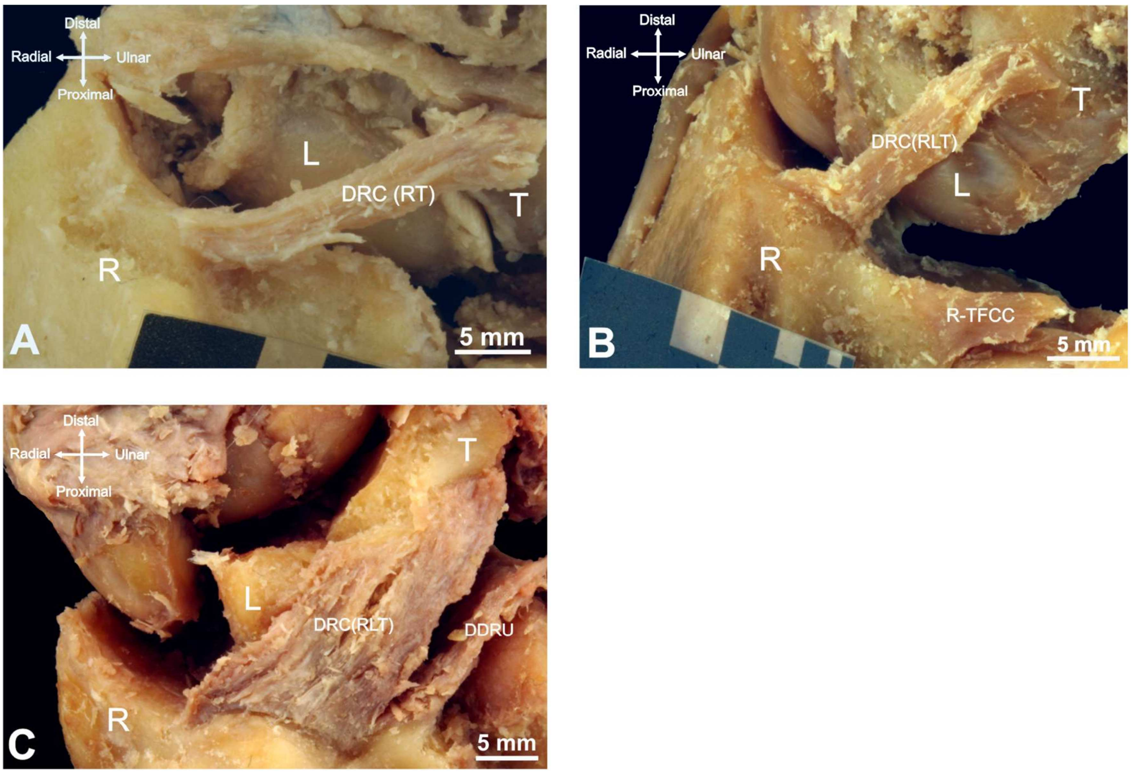

Figure 21. The dorsal radiocarpal ligament (DRC) configuration. **A**. RT configuration of the DRC attached over the middle of the distal end of the radius towards the triquetrum. **B.** Lunotriquetral band (RLT) of the DRC together with dorsal radio-triangular fibrocartilage complex ligament (R-TFCC). **C.** Very wide radiolunotriquetral of the DRC attached to the ulnar side of the radius adjacent to the dorsaldistal radioulnar ligament (DDRU). R= radius, L= Lunate, T= Triquetrum.

While a single banded DRC (n=7; 70 %) was dominated by the RLT configuration (n=5; 50%), a double-banded DRC (n=2; 20%) consisted of RT and RLT running together from the dorsal distal aspect of the radius towards the triquetrum in an arbitrary alignment (Figure 22). A triple banded DRC (n=1; 10%) was observed with a thin long RT on the ulnar side of the double RLTs running from the distal aspect of the radius and merging together as an inverted V-shape on the proximal dorsal aspect of the triquetrum (Figure 23).

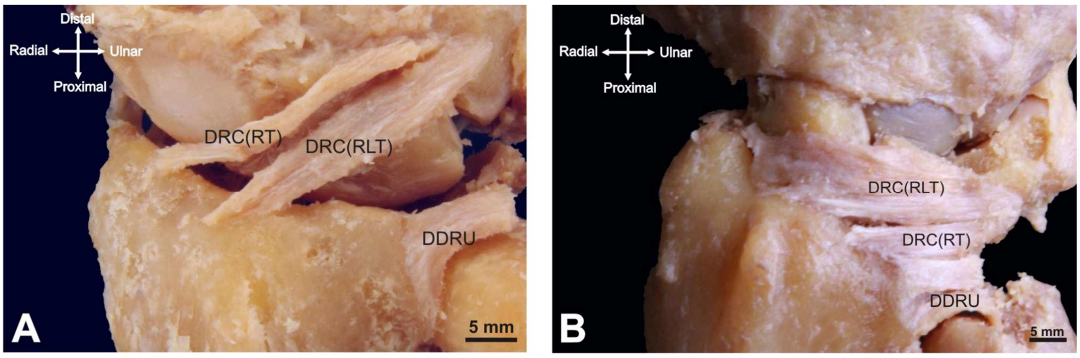

Figure 22. Double banded dorsal radiocarpal ligament (DRC) variations. **A.** Radiotriquetral band (RT) radial to the radiolunotriquetral band (RLT) and dorsal distal radioulnar ligament (DDRU). **B.** RT ulnar to RLT.

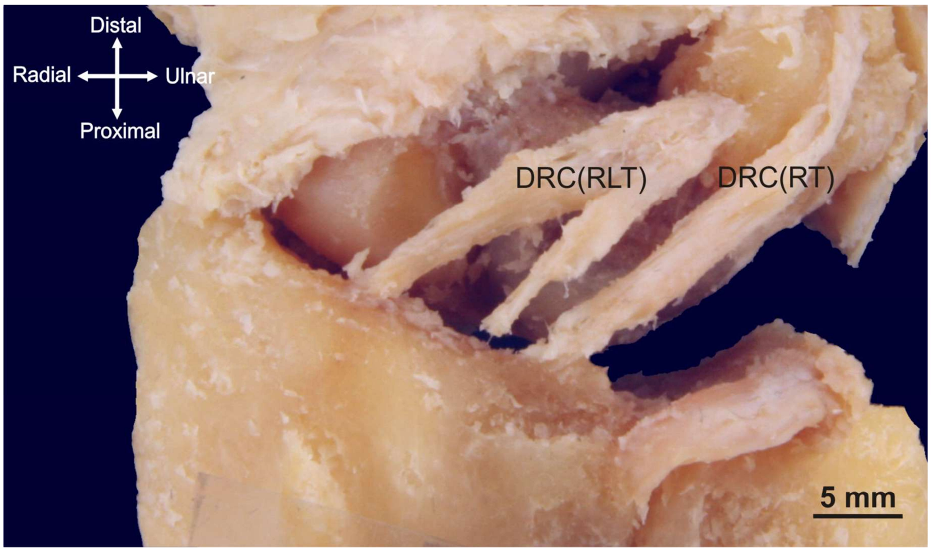

Figure 23. Triple dorsal radiocarpal ligament (DRC) structure, two radiolunotriquetral bands (RLT) just radial to radiotriquetral band (RT) and converging upon attaching to the triquetrum.

Accordingly, the RLT had a significantly greater mean surface area (159.6 ± 83.2 mm^2) than the RT (79.8 ± 33.7 mm^2; $p<0.05$). The RLT proximal (18.19 ± 22.20 mm^2) and distal (14.98 ± 10.63 mm^2) attachment areas showed insignificant difference with the RT proximal (16.36 ± 10.91 mm^2) and distal (10.63 ± 6.80 mm^2; $p>0.05$) attachments (Figure 24).

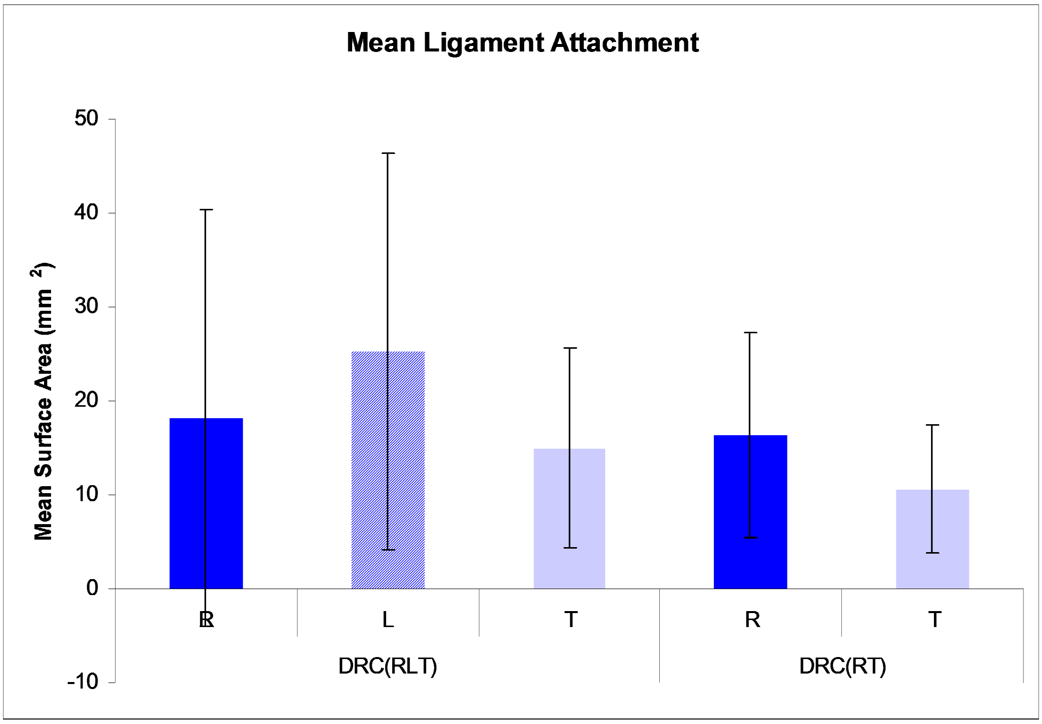

Figure 24. The dorsal radiocarpal ligaments (DRC) configuration mean osseous attachments. RLT=radiolunotriquetral band, RT=radiotriquetral band, R= radius, L= lunate and T= triquetrum, Scale bar= standard deviation.

2.3. Radioulnar and Radio-TFCC Ligaments:

The PDRU (n=8; 80%) was observed to span the area between the ulnar-most aspect of the radius and the ulna forming a ligamentous band that may share a connection with the TFCC (n=2; 20%) (Figure 25).

The DDRU (n=4; 40%) was identified as a discrete ligament attached between the dorsal aspect of the radius and ulna (Figure 26). However, it was often observed diverted into disorganised fibres within the TFCC, which hindered its isolation as a discrete ligament.

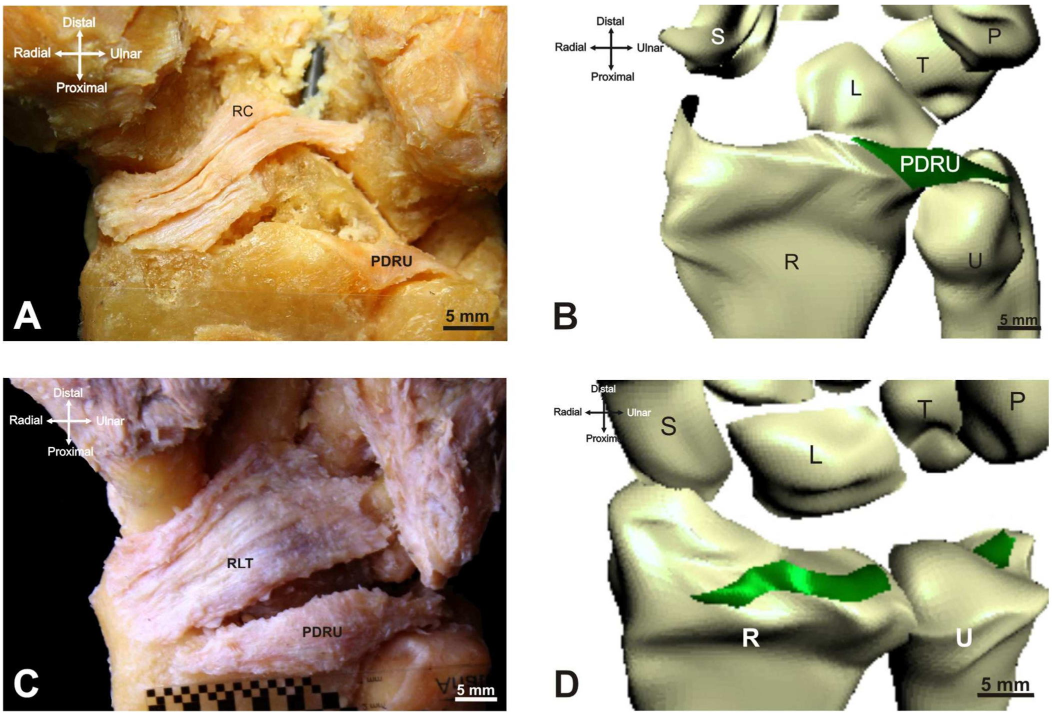

Figure 25. The palmar distal radioulnar ligament (PDRU) configuration. **A-B.** PDRU attached to the ulnar most aspect of the distal radius and tapered upon reaching the ulna. **C.** PDRU run from the middle of the distal aspect of the radius, expand in the middle and tapered on its distal attachment. **D.** Microscribe reconstruction of the same specimen with the actual ligamentous attachments. RC= radiocapitate ligament, RLT= radiolunotriquetral ligament, R=radius, U=ulna, S=scaphoid, L= lunate, T= triquetrum and P=pisiform.

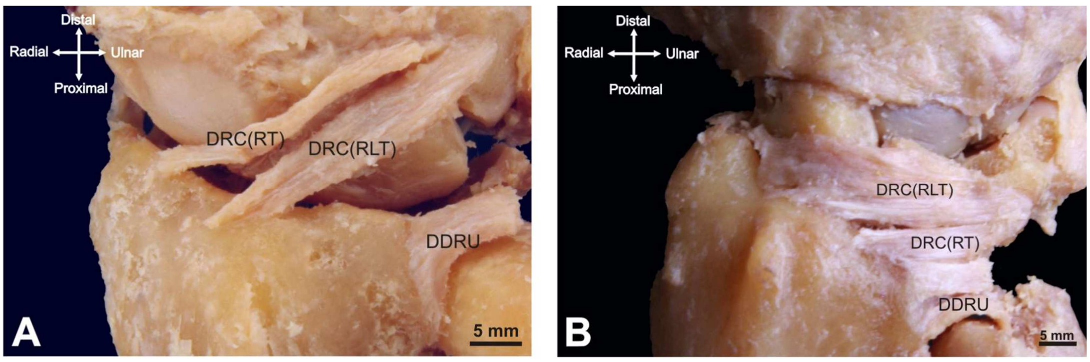

Figure 26. The dorsal distal radioulnar ligament (DDRU) variations. **A.** DDRU with triangular fibrocartilage complex (TFCC) connection. **B.** Discrete DDRU separated from radio-triangular fibrocartilage complex ligament (R-TFCC). DRC= dorsal radiocarpal ligament, RT= radiotriquetral band and RLT= radiolunotriquetral band.

The TFCC was shown to have various connections to the distal end of the radius and the radiocarpal ligaments. Although it was observed that the TFCC had a connection to the PDRU and DDRU, the more prominent attachment was found on the dorsal aspect of the distal end of the radius (n=5; 50%). A discrete palmar R-TFCC (n=1; 10%) linking the distal radius to the

TFCC was found to be interdigitated with the fibrous band of the dorsal R-TFCC (Figure 27). As a result, measurements were restricted to the Wp and Wm.

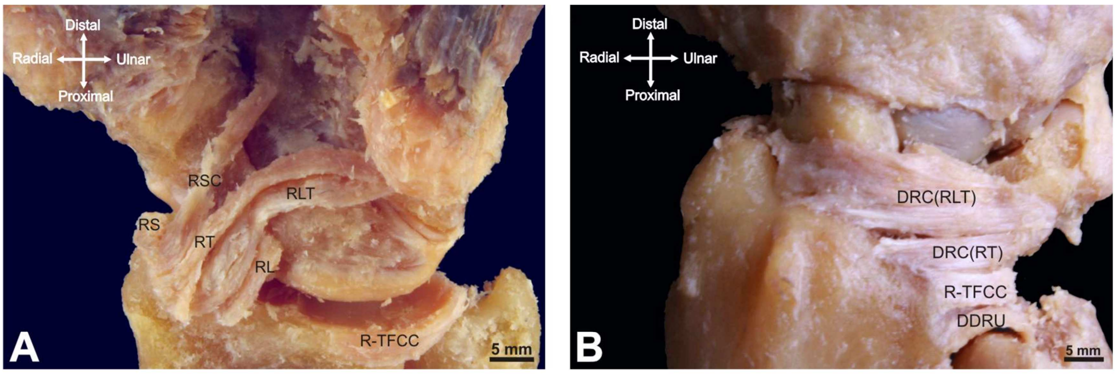

Figure 27. Palmar and dorsal radio-triangular fibrocartilage complex ligament (R-TFCC) structure. **A.** Palmar R-TFCC is continuous with dorsal R-TFCC attachment. **B.** Discrete dorsal R-TFCC radial to the dorsal distal radioulnar (DDRU). RS= radioscaphoid ligament, RSC= radioscaphocapitate ligament, RT= radiotriquetral ligament, RLT= radiolunotriquetral ligament, RL= radiolunate ligament, DRC= dorsal radiocarpal ligament, RT= radiotriquetral band and RLT= radiolunotriquetral band.

3. Histological Findings:

Among the four selected ligaments, the RSC and RLT radial attachment were damaged during the tissue preparation. While most of the ligaments had only one attachment on each bone included in their name, the RSC and RLT had proximal and distal attachments on the scaphoid and the lunate respectively (Figures 28 and 29).

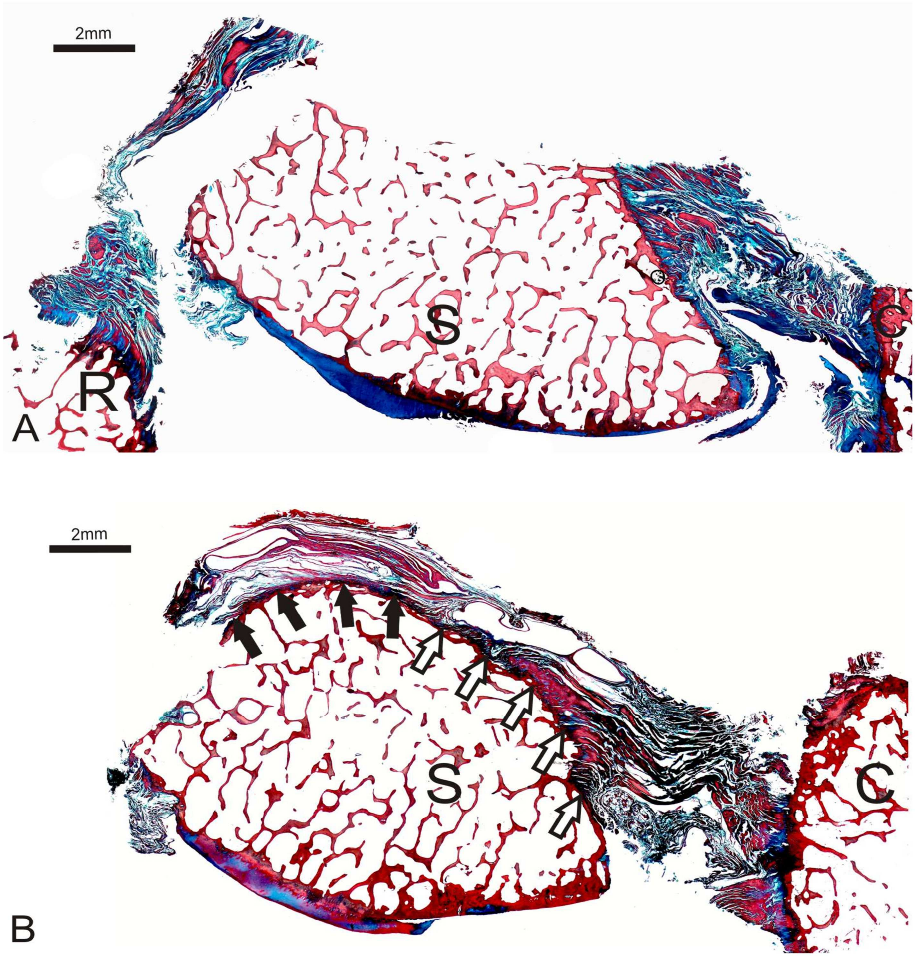

Figure 28.Section through the radioscaphocapitate ligament (RSC). **A.** Proximal (incomplete) and distal attachments. **B.** Proximal scaphoid attachment (Sp) (black arrows) and distal scaphoid attachment (Sd) (white arrows). R=radius, S=scaphoid and C= capitate.

The RSC had a greater enthesial bone index area (A/L) over the proximal scaphoid attachment (Sp) (149.48 ± 16.22 $\mu m^2/\mu m$), distal scaphoid attachment (Sd) (147.4 ± 22.77 $\mu m^2/\mu m$) and capitate (304.08 ± 39.68 $\mu m^2/\mu m$) than that of the capsular bone attachment (60.93 ± 2.39 $\mu m^2/\mu m$) (Figure 29). While the Sp of the RSC had a smaller enthesial bone index perimeter (P/L) (2.21 ± 0.06), the Sd (2.41 ± 0.05) and capitate (2.73 ± 0.24) enthesial bone P/L were greater than that of the capsular bone attachment (2.34 ± 0.007).

The RLT had a greater enthesial bone index area (A/L) on the proximal lunate attachment (Lp) (203.06 ± 36.25 $\mu m^2/\mu m$), distal lunate attachment (Ld) (251.61± 21.45 $\mu m^2/\mu m$) and triquetrum (148.81±16.22 μm^2/μm) than that of the capsular bone attachment. The RLT enthesial bone index perimeter (P/L) on the Lp (2.45 ± 0.04), Ld (2.24 ± 0.02) and triquetrum (2.63 ± 0.30) were greater than that of the capsular bone attachment (Figure 29).

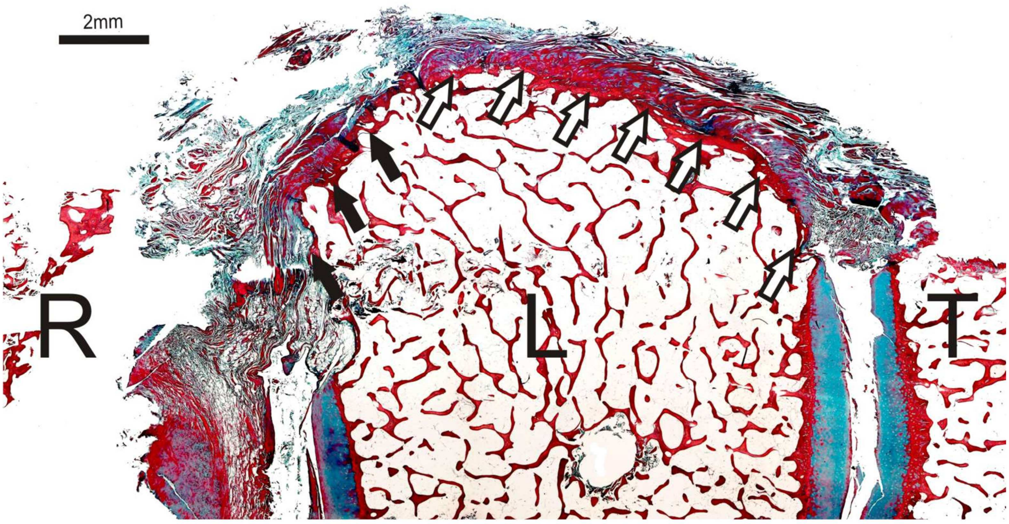

Figure 29. The radiolunotriquetral (RLT) osseous attachments: radial (missed), proximal lunate (Lp) (black arrows), distal lunate (Ld) (white arrows) and triquetrum attachments. R=radius, L=lunate and T=triquetrum.

The DRC had enthesial bone attachment on the radius and the triquetrum whereas it was attached to capsular bone on the lunate. The proximal and distal attachment of the DRC showed significant ligamentous attachments as the fascicles were spanned continuously from the radius toward the triquetrum. As a result, the mean DRC enthesial index area over the radius (282.90 ± 24.06 μm^2/μm) and the triquetrum (116.75 ± 24.90 μm^2/μm) were greater than that of the capsular bone attachment (60.93 ± 2.39 μm^2/μm) (Figure 30). Similarly, the DRC proximal (2.62 ± 0.32) enthesial bone index perimeter was greater than that of capsular bone attachment (2.34 ± 0.007), whereas its distal enthesial bone index perimeter (2.19 ± 0.10) was smaller than that of the capsular bone attachment.

Conversely, the DRC was identified to have attachment to the lunate with a loose connective tissue (to capsular bone), which suggested that this is not a mechanically significant attachment (Figure 30).

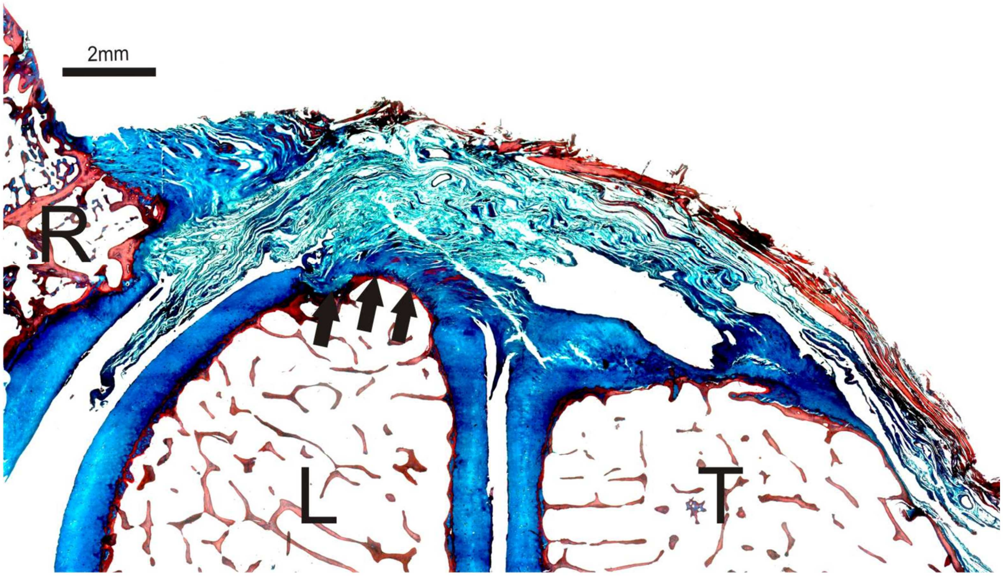

Figure 30. The dorsal radiocarpal ligament (DRC) radioluntriquetral band osseous attachments. The radial and triquetral attachments are considered as mechanically significant attachments (enthesial bone attachments) compared with the capsular attachment to the lunate (arrows). R=radius, L=lunate and T= triquetrum.

The PDRU had greater radial (293.69 ± 49.04 $\mu m^2/\mu m$) and ulnar (302.71± 50.82 $\mu m^2/\mu m$) enthesial bone index area than that of the joint capsule (Figure 31). Also, the PDRU was found to have greater proximal (2.41 ± 0.16) and distal (2.5 ± 0.11) enthesial bone index perimeter than that of the capsular bone attachment (2.34 ± 0.007).

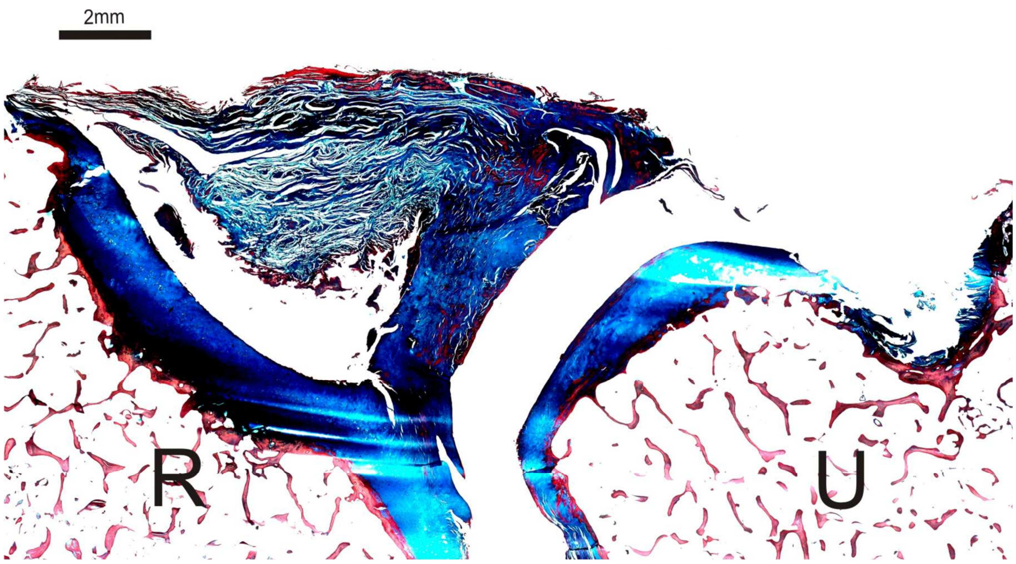

Figure 31. The palmar distal radioulnar ligament (PDRU) osseous attachments. R= radius and U= ulna.

Discussion

The lack of clear definition across the spectrum of wrist ligaments hindered the reproducibility of several studies. A lot of reports have mentioned the anatomy of the ligaments depending on gross dissection alone (Mayfield *et al.*, 1976; Berger and Landsmeer, 1990; Feipel and Rooze, 1999; Theumann *et al.*, 2003; Nagao *et al.*, 2005). Manual measurement has been widely adopted (Feipel and Rooze, 1999; Viegas *et al.*, 1999; Nagao *et al.*, 2005). The current study suggests that this is not the most reliable method. Furthermore, there were no consistent comparisons between the various sets of measurements or any detailed statistical analyses. The current study considered the variability as well as the diversity of each ligament attachment. Also, the measurement technique was done in a way to more precisely represent the shape of each ligament, which enhances the reproducibility of the data. Three different levels of the length (Lr, Lm and Lu) and width (Wp, Wm and Wd) were measured for each ligament as the length or width of each ligament may not be similar over the entire structure. Considering intra-observer variation, the measurements were repeated twice by the same observer (R.A.); statistically significant ($p<0.05$) differences between rounds of measurement were considered inaccurate. The current study demonstrated that the entire described ligament showed a high variability. For example, the mean DRC (RLT) proximal attachment area (18.19 mm^2) was smaller than the standard deviation (22.20 mm^2) which reflected that further classification into distinct subtypes might be needed (Figure 24).

Among the three methods of measurements that were included in the current study, the most accurate and reproducible was with the microscribe. Unlike using callipers and digital image software, there were no significant inconsistencies between the rounds of measurements with this instrument. It was observed that there was no statistically significant difference between the rounds of measurement for each method when measuring planar ligaments (Figure

9). However, the microscribe method was the most reproducible method when considering multi-planar ligaments, which were harder to reach with the callipers or to visualise photographically in a measurable plane for its entire dimensions (Figure 10). Accordingly, there was no significant difference between the rounds of measurement with the microscribe method during the measurement of all ligaments ($p>0.05$) while the manual and digital methods showed a significant difference in multi-planar ligaments measurements ($p<0.05$).

Obtaining accurate and reproducible calliper and digital image measurements were hindered by the palmar projections of the walls of the carpal tunnel that obscure the access or vision. Whenever there is no access to use the digital microscribe, cutting the palmar projections of the carpal tunnel may result in more accurate and consistent measures with calliper and digital image software measurement.

In addition to using an accurate method for measurements, indexing the measurements may further enhance the reproducibility of the results and may decrease the comparative inconsistencies in the literature. Indexing of the results (e.g. against metacarpal length) may facilitate the comparison between studies and omit the individualised specimen variability in regards to the size of the hand, gender, occupation, etc. The current study reinforces the need for this approach, which will be applied to future studies.

Two different types of radiocapitate ligaments were reported in the literature but there were no clear reports about the various modes of attachments (Figure 1). The first type is the RC that was found to proximally attach to the radial styloid process. Then, it coursed distally to attach to the medial aspect of the scaphoid. Its distal insertion was reported to be on the lateral aspect of the body of the capitate (Mayfield *et al.*, 1976; Berger and Blair, 1984; Berger *et al.*, 1984). This anatomical description is confirmed by the current study findings, but no quantitative description was discussed and therefore cannot be compared with the current study's data directly.

A further study presented morphometric data of the RC including details of the length and width manually measured at three different levels (Feipel and Rooze, 1999). The study adopted a similar technique of manual measurement to the current study but reported longer mean manual Lr, Lm and Lu than that of the current study. Similarly, the study showed greater mean manual Wp, Wm, and Wd than the current study. The ligamentous surface area was calculated using measurement data of the length and width but no ligamentous attachment analyses were included. Also, the mean RC surface area was greater than that of the current study. Differences between this study and the current study may be due to a lack of clear definition of a ligament, and distinct identification of the endpoints by removing the periosteum. The current study achieves reproducible results because the attachments are clearly defined. The current study therefore provides a clear and complete quantitative analysis of the ligamentous dimensions and osseous attachments (Figures 12 and 14). Such variability among the few previous quantitative studies may also be attributed to the use of absolute measurements rather than index measurements. Specimens in each sample population are likely to be widely different in general size (big / small hands), providing an obvious reason for the discrepancies. This again advocates use of index measures in future studies.

The second type of radiocapitate ligament is the RSC. It was reported to be the radial-most of the palmar radiocarpal ligaments (Berger and Landsmeer, 1990). This was confirmed by the current study, except when a radioscaphoid connection existed (Figure 13). Several authors' investigations regarding the proximal attachment of the RSC suggested that it extended from the styloid process of the radius towards the scaphoid fossa distal to the scaphoid waist (Berger and Landsmeer, 1990; Theumann *et al.*, 2003; Kijima and Viegas, 2009). The current study revealed a similar description of the proximal RSC attachment (Figures 13 and 14). The ligamentous fibres of the RSC that arise from the distal-most part of the radial styloid process have been described to extend towards the waist of the scaphoid and form what is known as the RCL (Berger and Landsmeer, 1990). No discrete RCL was identified by the current study. Further investigations should be directed towards proving whether or not the RCL exists as described in the literature (Mayfield *et al.*, 1976; Mizuseki and Ikuta, 1989; Berger and Landsmeer, 1990).

There were inconsistencies between papers when considering the distal attachments of the RSC. It has been reported that the distal attachment of the RSC was in the centre of the palmar surface of the capitate (Theumann *et al.*, 2003; Kijima and Viegas, 2009). Conversely, it was found that most RSC fibres are not inserted on the body of the capitate, rather just a reflection of the synovial stratum covering the ligamentous fibres inserted over the body of the capitate (Berger and Landsmeer, 1990). However, the current study confirmed that ligamentous fibres of the RSC did attach to the centre of the palmar aspect of the capitate, and provided further confirmation histologically (Figures 13 and 28).

In addition to the RC and RSC, a third mode of the radiocapitate connection was identified in the current study, RSC-T. The RSC-T was attached to the radial styloid process, the scaphoid, central surface of the capitate and the radial aspect of the triquetrum (Figure 13). Also, it may give attachment to the hamate (Figure 15). This has not been identified in the reviewed literature.

Variability in radiocapitate ligamentous connections suggests variable carpal biomechanics. The RC acts like a sling, which may restrain scaphoid extension by limiting the palmar movement of the proximal pole of the scaphoid. In addition, the RC may facilitate the rotation of the scaphoid by acting as a pulley (Fogg, 2004). Conversely, the RSC may resist the rotation of the scaphoid and facilitate flexion-extension motions. Accordingly, the RC indicates that the scaphoid may be rotated while the RSC may act in favour of flexed/extended scaphoid (Fogg, 2004). Further work is needed to test the mechanical effects of these anatomical sub-types. Functional correlations with anatomical variation such as this may be important for more individualised diagnosis and treatment of wrist dysfunction.

The current study confirmed that there was a true ligamentous connection between the radius and the scaphoid but there was no connection to the lunate composed of parallel and organised fascicles. Accordingly, a discrete RS consisted of fasciculated collagen fibres was identified on the radial-most aspect of the wrist between the styloid process of the radius, the scaphoid, and may also attach to the trapezium (Figure 16). It is different than what was described in the literature as a vertical neurovascular bundle (Berger and Landsmeer, 1990) as it was occupying the radial-most margin of the wrist rather than being between the scaphoid and the lunate. This difference may be of importance surgically as it may be a key contributor to neurovasculature of the proximal wrist and may need to be preserved. Further studies of the wrist neurovasculature may clarify this.

The variability of the attachment between the radius and the lunate was explained in several papers (Berger and Landsmeer, 1990; Berger, 1997; Feipel and Rooze, 1999; Theumann *et al.*, 2003; Nagao *et al.*, 2005; Kijima and Viegas, 2009). The RL, LRL, SRL and RLT were reported in the literature to be the main ligaments representing the connection between the radius and the lunate. The RLT or RT is also referred to in the literature as the " long radiolunate ligament" (Lewis *et al.*, 1970; Mayfield *et al.*, 1976; Taleisnik, 1976; Theumann *et al.,* 2003). However, a discrete RT ligament was described from the radial styloid process towards the palmar surface of the triquetrum and had a lunate attachment as well (Mayfield *et al.*, 1976). The current study showed that the RLT and RT could both exist as discrete ligaments along with the

RL in the same specimen (Figure 18). Also, the RLT was identified together with the LRL and SRL in the same specimen (Figure 17). As a result, the current study suggested that the RLT and RT shouldn't be used as synonyms of the LRL.

Variability of radiolunate connections had been previously quantified (Feipel and Rooze, 1999). While the double configuration may be referred to as the LRL and SRL (Berger and Landsmeer, 1990; Berger, 1997; Nagao *et al.*, 2005; Kijima and Viegas, 2009), it was suggested that the single and double radiolunate connection configurations were single and double RL respectively (Feipel and Rooze, 1999). Although the ligamentous description of the double RL configuration suggested the LRL and SRL morphology described elsewhere in the literature, it was described as double RL configuration without any specification. The current study suggests that a single radiolunate connection is better referred to as a RL, and the double configuration showed different morphology, so LRL and SRL is a better description (Figure 16). Moreover, the study followed a similar technique of manual measurement adopted by the current study but there was neither another method of measurement, nor a study of the ligamentous attachment. The study reported shorter mean manual Lr than that of the current study. Conversely, the mean manual Lm and Lu as well as the mean surface area of the RL were reported to be greater than that of the current study. Also, the study showed greater mean manual Wp, Wm and Wd than the current study. The study did not include a clear description of the ligamentous identification. The current study, however, depends on strict criteria of dissection in addition to the histological analysis that favours the accuracy and reproducibility of the results.

Another quantitative study of radiocarpal ligaments provided manual measurements of the ligaments around the lunate but without any details about the technique of measurement (Nagao *et al.*, 2005). Unlike the current study, this study showed only one length and width for each ligament, which hinders a direct comparison with the current study's data. There were clear differences between the reported ligamentous bony attachments and the current study findings. The mean proximal and distal LRL attachments were reported to be much smaller than what was found in the current study. Also, the SRL was reported to have a greater proximal attachment area but smaller distal attachment area than the current study. It was also unclear how ligamentous tissue was defined in the earlier study.

The variation in the radiolunate connection configuration suggests a functional differentiation. It opens the door for a further investigation of the mechanical variations to determine whether or not a second radiolunate connection (i.e. the SRL) may influence the lunate motion during flexion-extension as well as radial/ulnar deviation (Feipel and Rooze, 1999). These ligamentous differences may also be associated with variable lunate types (Fogg, 2004). Future studies should combine data on carpal bone morphology and ligament patterns to ascertain the structural basis for variable motion patterns.

The DRC is also reported in the literature as the radiotriquetral ligament and the radiolunotriquetral ligament (Feipel and Rooze, 1999; Viegas *et al.*, 1999; Viegas, 2001). Although there were inconsistencies between investigators' results regarding the DRC attachments (Figure 2), its proximal and distal attachments were consistently described to be on the dorsal aspect of the radius and the dorsal tubercle of the triquetrum respectively (Mizuseki and Ikuta, 1989; Berger, 1997; Feipel and Rooze, 1999; Viegas *et al.*, 1999; Theumann *et al.*, 2003; Kijima and Viegas, 2009). The DRC attachment to the lunate was not confirmed in all papers (Feipel and Rooze, 1999; Theumann *et al.*, 2003). The current study combines both ideas regarding the DRC configuration, which could be either RT or RLT (Figures 21, 24 and 30).

Based on the DRC classification (Figure 3), type I DRC matches what was found in the current study regarding the single-banded DRC (Figure 21). Type II and type III DRC was not confirmed in the current study. Type IV DRC is more consistent with the double-banded DRC configuration described in the current study (Figure 22). In the current study, however, no obvious classification could be obtained due to the limitation of the number of the specimens included in the study.   A larger sample size may bring these differences to light.

A morphological analysis of the capsular ligaments of the wrist suggested that the DRC is formed by radiotriquetral ligamentous configuration and no lunate attachment was identified (Feipel and Rooze, 1999). Among the 66 specimens that were studied; single, double and triple configurations were identified in 36%, 52% and 13 % respectively (Feipel and Rooze, 1999). The current study identified that the DRC is made of two modes of ligamentous configuration, the RT and RLT bands, which can be single banded (70%), arranged in double (20%), or even triple banded (10%) manners (Figures 21,22 and 23). The single banded RLT was the commonest among all patterns but further investigations are needed to confirm this because of the limited sample of the current study. Besides the DRC configuration, the study added morphometric data on the DRC (RT) with a similar technique followed by the current study but without ligamentous attachment data (Feipel and Rooze, 1999). The study followed a similar technique of manual measurement of the current study but reported shorter mean manual Lr than that of the current study. Conversely, the mean manual Lm, Lu, Wp, Wm and Wd were reported to be greater than that of the current study. These differences again highlight the need for consistent ligament definition, technique description and indexing of measures against hand size.

The DRC configuration has been previously described to include superficial and deep parts (Shaaban and Lees, 2006). The superficial ulnar part ran from the distal interosseous border of the radius obliquely and ulnarly to the lunate and triquetrum. Similarly, the deep radial part of the ligament ran ulnarly from the posterior border of the radius almost horizontally to terminate on the lunate and triquetrum (Shaaban and Lees, 2006). These arrangements were not observed in the current study.

The DRC together with the dorsal intercarpal ligament (DIC) was demonstrated to have a lateral V configuration that indirectly provides radioscaphoid stability (Viegas *et al.*, 1999). Working together with the dorsal intercarpal interosseous ligaments of the proximal carpal row, the DRC and DIC allow the angle between the two arms of the V to change, stabilizing the proximal pole of the scaphoid throughout global wrist motion (Viegas *et al.*, 1999). In addition, it might also limit midcarpal joint rotation (Berger, 1997). Loss of the integrity of the DRC was found to result in a non-dissociative static PISI (Viegas *et al.*, 1999). Considering the configuration of the DRC demonstrated by the current study, a double or triple DRC pattern might strengthen the joint and resist static PISI deformity, particularly if a single band were disrupted. Further biomechanical investigation should be carried out in order to determine the biomechanical stability of such configuration in prevention of carpal instability. A retrospective radiologic study may also determine a link with ligament type and susceptibility to PISI, should sufficient MRI detail be available.

The current study is supported by the histological investigation of the entheses. Each ligamentous structure was meticulously dissected by following the fascicular pattern over the entire length. Then, studying the entheses confirmed the finding of the dissection and favoured the reproducibility and accuracy of the study (Figures 28, 29, 30 and 31). The mechanical role of each ligament is suggested by larger areas of bone where they were attached (enthesial bone). Poorly organised (true capsular) tissue was attached to significantly smaller areas of bone (capsular bone) (Fogg *et al.*, 2005), suggesting less force transfer than the enthesial bone. With this approach, the current study was able to not only demonstrate the attachment of specific bands to bone (or not), but to also provide a quantitative indication of each ligament’s function. Further investigation is needed to determine the effects of such attachments in the biomechanics of the wrist joint with relation to carpal instability (Figure 30). It is hoped that a complete enthesial survey of the wrist will inform the allocation of mechanical necessity to individual ligaments, i.e. which are most important to retain/restore surgically.

The current study had a number of limitations. The sample size was comparable to that of other studies, but too small to give a clear indication of subtype frequency. A larger study following the procedures described here is recommended. Despite demonstrating its accuracy and reproducibility against digital and manual measurements, the microscribe may be subject to observer error. The device is capable of resolving points 0.1mm apart, but when done with the naked eye this resolution is not possible. The likelihood of error is largely mitigated by repeated measures and their positive analyses, but multiple observers and increased round numbers may increase confidence in the results of future studies. Histological proofs for each ligament should be provided in future studies.

Understanding the variability of the wrist ligament anatomy results in better understanding of wrist instability (Dias and McMohan, 1988; Garcia-Elias *et al.*, 1989; Dobyns and Gabel, 1990; Herzberg *et al.*, 1993; Viegas *et al.*, 1995). A comprehensive knowledge of carpal instability of the wrist is hindered by the complex anatomy and kinematics as well as the various patterns of injury (Mayfield *et al.*, 1980; Wiesner *et al.*, 1996; Carlsen and Shin, 2008; Kuo and Wolfe, 2008). This explains why it is worth knowing that the various configuration of each ligament may play a role in the determination of the outcome, considering the impact and the consequences of an injury (Dias and McMohan, 1988; Dobyns and Gabel, 1990; Viegas, 1998; Linscheid *et al.*, 2002). The current study suggests that a clear understanding of various patterns of the radiocarpal ligaments is important for the sake of accurate management and may lead to better aetiological investigations. In addition, the current study provided quantitative details of the variable ligamentous attachments. Measurement of each ligamentous dimension and osseous attachments supported by a histological analysis were also included. This may be a useful guide for better understanding of carpal instability and proper management.

Conclusion

The current study demonstrates that the radiocarpal ligament configuration is highly variable. In order to obtain reproducible data, strict criteria should be followed with a clear definition of the ligament as a structure. It is suggested to use the microscribe to get the best record of ligamentous dimensions. The findings of the current study will provide insight when considering the complex anatomy of the radiocarpal ligaments and their osseous attachment in relation to carpal instability aetiology and management. Further studies are required to determine the relative link between gender, race and/or occupation and morphological variability, and to address the mechanical significance of each variant.

Appendix 1 - Tissue Preparation and Staining for Light Microscopy

Quentin A. Fogg BSc; Scaphotrapeziotrapezoidal Joint Anatomy and Degenerative Arthritis; 1999 Honours Thesis

Accelerated Decalcification

Ingredients: **WEAR GLOVES WHEN PREPARING THIS**

1% EDTA
9.5% nitric acid (HNO_3)
Distilled H_2O

Double-Embedding

This double-embedding procedure was adopted to combat the difficulties faced with the traditional single-embedding procedure. The double-embedding procedure was as follows:

50% alcohol *all day*

70% alcohol *overnight*

95% alcohol *all day*

Absolute alcohol *1.5 hours, then change for overnight*

50% alcohol: 50% diethyl-ether *half day* **IN FUMEHOOD**

1% cellulose nitrate in 50% alcohol: 50% diethyl ether *half day, overnight, half day* **IN FUMEHOOD**

Chloroform *2 hours* **IN FUMEHOOD**

Dry on paper **IN FUMEHOOD**

Immerse in liquid paraffin wax *20 minutes* **IN FUMEHOOD**

Vacuum to 15Pa in liquid paraffin wax *30 minutes* TEST

Vacuum to 20-25Pa in liquid paraffin wax *2 x 1.5 hours* TEST

Slide Coating and Weighting **OPTIONAL**

To facilitate section adhesion to the slides each slide was coated with a gelatine mixture.

Solution

2.5g gelatine

0.25g chromium III potassium sulphate ($CrK(SO_4)_2\ 12H_2O$)

500mL distilled water

Gelatine dissolved into 250mL distilled water on medium heat with stirrer

Chromium dissolved in 250mL of distilled water

Gelatine solution added to chromium solution through filter paper.

Procedure

Slides were cleaned with soapy water

Rinsed in warm water

Placed in warm gelatine solution and carefully removed to avoid creating bubbles on the slide surface.

Placed in oven (50^0 C) overnight

Sealed in airtight container until used

Modified Masson's Trichrome Staining

Ingredients

Ponceau de xylidine Phosphomolybdic acid

Acid fuchsin

Glacial acetic acid

Light green SF

Wiegert's A and B[1] **USE MAYER'S IF AVAILABLE**

Hydrochloric acid

[1] Mixed solutions of Wiegert's A and B will only last for 2 days

Stains

1. Cytoplasmic Red **

A = 1% ponceau de xylidine in 1% acetic acid

B = 1% acid fuchsin in 1% acetic acid

Mix together in a ration of 2A: 1B

To make 300mL

A = 2g ponceau de xylidine + 2mL acetic acid in 200ml H_2O

B = 1g acid fuchsin + 1mL acetic acid in 100mL H_2O

The final pH ≈ 3.05

2. Light Green

2g Light Green SF + 2mL acetic acid + 100mL H_2O

Final pH ≈ 2.85

Procedure

1. Dewax in HistoClear for 15 minutes

2. Bring sections to water using the following sequence:

Absolute Alcohol	2 minutes
Absolute Alcohol	2 minutes
90% Alcohol	2 minutes
70% Alcohol	4 minutes
Rinse in running water	4 minutes

**Alternative technique or go below to step 3:

> **Stain in Wiegert's Haematoxylin (A +B) for 5 minutes
>
> **Rinse in tap water
>
> **Differentiate in 1% HCl (2-3 quick dips)

3. Stain in Mayer's Haematoxylin 8 minutes

4. Blue in running tap water for approx. 10 minutes

Check that only nuclei are stained

5. Stain in Cytoplasmic Red for 1 minute

6. Rinse in two washes (dips) of 1% acetic acid

7. Displace in 4% phosphomolybdic acid for 2 minutes

8. Rinse in 1 wash of 1% acetic acid

9. Stain with Light Green for 35-70 seconds (may have to vary time)

10. Rinse in 1 wash of 1% acetic acid

11. Blot, and then dehydrate using the following sequence:

70% Alcohol	1 minute
90% Alcohol	1 minute
Absolute Alcohol	2 minutes
Absolute Alcohol	3 minutes

12. Clear in HistoClear for 5 minutes

13. Mount slides in DPX (mounting medium) **<u>IN FUMEHOOD</u>**

References

Benjamin, M., E. J. Evans and L. Copp (1986). "The histology of tendon attachments to bone in man." J Anat **149**: 89-100.

Benjamin, M. and D. McGonagle (2001). "The anatomical basis for disease localisation in seronegative spondyloarthropathy at entheses and related sites." J Anat **199**(Pt 5): 503-26.

Benjamin, M. and D. McGonagle (2009). "Entheses: tendon and ligament attachment sites." Scand J Med Sci Sports **19**(4): 520-7.

Benjamin, M., B. Moriggl, E. Brenner, P. Emery, D. McGonagle and S. Redman (2004). "The "enthesis organ" concept: why enthesopathies may not present as focal insertional disorders." Arthritis Rheum **50**(10): 3306-13.

Benjamin, M. and J. R. Ralphs (1998). "Fibrocartilage in tendons and ligaments--an adaptation to compressive load." J Anat **193 (Pt 4)**: 481-94.

Benjamin, M., H. Toumi, J. R. Ralphs, G. Bydder, T. M. Best and S. Milz (2006). "Where tendons and ligaments meet bone: attachment sites ('entheses') in relation to exercise and/or mechanical load." J Anat **208**(4): 471-90.

Berger, R. A. (1997). "The ligaments of the wrist. A current overview of anatomy with considerations of their potential functions." Hand Clin **13**(1): 63-82.

Berger, R. A. (2001). "The anatomy of the ligaments of the wrist and distal radioulnar joints." Clin Orthop Relat Res(383): 32-40.

Berger, R. A. and W. F. Blair (1984). "The radioscapholunate ligament: a gross and histologic description." Anat Rec **210**(2): 393-405.

Berger, R. A., W. F. Blair and G. Y. El-Khoury (1984). "Arthrotomography of the wrist. The palmar radiocarpal ligaments." Clin Orthop Relat Res(186): 224-9.

Berger, R. A. and J. M. Landsmeer (1990). "The palmar radiocarpal ligaments: a study of adult and fetal human wrist joints." J Hand Surg Am **15**(6): 847-54.

Camus, E. J., F. Millot, J. Lariviere, S. Raoult and M. Rtaimate (2004). "Kinematics of the wrist using 2D and 3D analysis: biomechanical and clinical deductions." Surg Radiol Anat **26**(5): 399-410.

Carlsen, B. T. and A. Y. Shin (2008). "Wrist instability." Scand J Surg **97**(4): 324-32.

Dias, J. J. and A. McMohan (1988). "Effect of Colles' fracture malunion on carpal alignment." J R Coll Surg Edinb **33**(6): 303-5.

Dobyns, J. H. and G. T. Gabel (1990). "Gymnast's wrist." Hand Clin **6**(3): 493-505.

Feipel, V. and M. Rooze (1999). "The capsular ligaments of the wrist: morphology, morphometry and clinical applications." Surg Radiol Anat **21**(3): 175-80.

Fogg, Q. A. (2004). Scaphoid Variation and an Anatomical Basis for Variable Carpal Mechanics. Department of Anatomical Sciences. Adelaide, The University of Adelaide. **PhD:** 275.

Fogg, Q. A., M. Loukas and R. A. Tedman (2005). "Determination and Analysis of Enthesial and Paraenthesial Bome in the Wrist; Are histological data relatable to computed tomographic images?" Surgical and Radiologic Anatomy **27**: S132-133.

Galtes, I., A. Rodriguez-Baeza and A. Malgosa (2006). "Mechanical morphogenesis: a concept applied to the surface of the radius." Anat Rec A Discov Mol Cell Evol Biol **288**(7): 794-805.

Garcia-Elias, M., J. H. Dobyns, W. P. Cooney, 3rd and R. L. Linscheid (1989). "Traumatic axial dislocations of the carpus." J Hand Surg Am **14**(3): 446-57.

Herzberg, G., J. J. Comtet, R. L. Linscheid, P. C. Amadio, W. P. Cooney and J. Stalder (1993). "Perilunate dislocations and fracture-dislocations: a multicenter study." J Hand Surg Am **18**(5): 768-79.

Kawamura, K. and K. C. Chung (2007). "Management of wrist injuries." Plast Reconstr Surg **120**(5): 73e-89e.

Kijima, Y. and S. F. Viegas (2009). "Wrist anatomy and biomechanics." J Hand Surg Am **34**(8): 1555-63.
Kuo, C. E. and S. W. Wolfe (2008). "Scapholunate instability: current concepts in diagnosis and management." J Hand Surg Am **33**(6): 998-1013.
Lewis, O. J., R. J. Hamshere and T. M. Bucknill (1970). "The anatomy of the wrist joint." J Anat **106**(Pt 3): 539-52.
Linscheid, R. L., J. H. Dobyns, J. W. Beabout and R. S. Bryan (2002). "Traumatic instability of the wrist: diagnosis, classification, and pathomechanics." J Bone Joint Surg Am **84-A**(1): 142.
Majima, M., E. Horii, H. Matsuki, H. Hirata and E. Genda (2008). "Load transmission through the wrist in the extended position." J Hand Surg Am **33**(2): 182-8.
Mayfield, J. K., R. P. Johnson and R. F. Kilcoyne (1976). "The ligaments of the human wrist and their functional significance." Anat Rec **186**(3): 417-28.
Mayfield, J. K., R. P. Johnson and R. K. Kilcoyne (1980). "Carpal dislocations: pathomechanics and progressive perilunar instability." J Hand Surg Am **5**(3): 226-41.
McLean, J. M., P. C. Turner, G. I. Bain, N. Rezaian, J. Field and Q. Fogg (2009). "An association between lunate morphology and scaphoid-trapezium-trapezoid arthritis." J Hand Surg Eur Vol **34**(6): 778-82.
Mizuseki, T. and Y. Ikuta (1989). "The dorsal carpal ligaments: their anatomy and function." J Hand Surg Br **14**(1): 91-8.
Nagao, S., R. M. Patterson, W. L. Buford, Jr., C. R. Andersen, M. A. Shah and S. F. Viegas (2005). "Three-dimensional description of ligamentous attachments around the lunate." J Hand Surg Am **30**(4): 685-92.
Nanno, M., R. M. Patterson and S. F. Viegas (2006). "Three-dimensional imaging of the carpal ligaments." Hand Clin **22**(4): 399-412; abstract v.
Nanno, M. and S. F. Viegas (2009). "Three-dimensional computed tomography of the carpal ligaments." Semin Musculoskelet Radiol **13**(1): 3-17.
Palmer, A. K., J. H. Dobyns and R. L. Linscheid (1978). "Management of post-traumatic instability of the wrist secondary to ligament rupture." J Hand Surg Am **3**(6): 507-32.
Reagan, D. S., R. L. Linscheid and J. H. Dobyns (1984). "Lunotriquetral sprains." J Hand Surg Am **9**(4): 502-14.
Shaaban, H. and V. C. Lees (2006). "The two parts of the dorsal radiocarpal (radiolunotriquetral) ligament." J Hand Surg Br **31**(2): 213-5.
Shin, A. Y., M. J. Battaglia and A. T. Bishop (2000). "Lunotriquetral instability: diagnosis and treatment." J Am Acad Orthop Surg **8**(3): 170-9.
Short, W. H., F. W. Werner, J. K. Green and S. Masaoka (2005). "Biomechanical evaluation of the ligamentous stabilizers of the scaphoid and lunate: Part II." J Hand Surg Am **30**(1): 24-34.
Taleisnik, J. (1976). "The ligaments of the wrist." J Hand Surg Am **1**(2): 110-8.
Taleisnik, J. (1984). "Classification of carpal instability." Bull Hosp Jt Dis Orthop Inst **44**(2): 511-31.
Tang, J. B. (2008). "General concepts of wrist biomechanics and a view from other species." J Hand Surg Eur Vol **33**(4): 519-25.
Theumann, N. H., C. W. Pfirrmann, G. E. Antonio, C. B. Chung, L. A. Gilula, D. J. Trudell and D. Resnick (2003). "Extrinsic carpal ligaments: normal MR arthrographic appearance in cadavers." Radiology **226**(1): 171-9.
Trail, I. A., J. K. Stanley and M. J. Hayton (2007). "Twenty questions on carpal instability." J Hand Surg Eur Vol **32**(3): 240-55.
Viegas, S. F. (1998). "Ulnar-sided wrist pain and instability." Instr Course Lect **47**: 215-8.
Viegas, S. F. (2001). "The dorsal ligaments of the wrist." Hand Clin **17**(1): 65-75, vi.
Viegas, S. F., R. M. Patterson and K. Ward (1995). "Extrinsic wrist ligaments in the pathomechanics of ulnar translation instability." J Hand Surg Am **20**(2): 312-8.

Viegas, S. F., S. Yamaguchi, N. L. Boyd and R. M. Patterson (1999). "The dorsal ligaments of the wrist: anatomy, mechanical properties, and function." J Hand Surg Am **24**(3): 456-68.
Wiesner, L., C. Rumelhart, E. Pham and J. J. Comtet (1996). "Experimentally induced ulno-carpal instability. A study on 13 cadaver wrists." J Hand Surg Br **21**(1): 24-9.